



ELSEVIER

Contents lists available at ScienceDirect

Deep-Sea Research II

journal homepage: www.elsevier.com/locate/dsr2

The carbon dioxide system and net community production within a cyclonic eddy in the lee of Hawaii

Feizhou Chen^a, Wei-Jun Cai^{a,*}, Yongchen Wang^a, Yoshimi M. Rii^b,
Robert R. Bidigare^b, Claudia R. Benitez-Nelson^c

^a Department of Marine Sciences, University of Georgia, Athens, GA 30602-3636, USA

^b Department of Oceanography, University of Hawaii at Manoa, Honolulu, HI 96822, USA

^c Department of Geological Sciences/Marine Sciences Program, University of South Carolina, Columbia, SC 29208, USA

ARTICLE INFO

Article history:

Accepted 18 January 2008

Available online 7 May 2008

Keywords:

Mesoscale processes

Cyclonic eddies

Dissolved inorganic carbon (DIC)

Net community production (NCP)

Subtropical North Pacific Ocean

E-Flux

ABSTRACT

The dynamics of dissolved inorganic carbon (DIC) and processes controlling net community production (NCP) were investigated within a mature cyclonic eddy, Cyclone *Opal*, which formed in the lee of the main Hawaiian Islands in the subtropical North Pacific Gyre. Within the eddy core, physical and biogeochemical properties suggested that nutrient- and DIC-rich deep waters were uplifted by ~80 m relative to surrounding waters, enhancing biological production. A salt budget indicates that the eddy core was a mixture of deep water (68%) and surface water (32%). NCP was estimated from mass balances of DIC, nitrate+nitrite, total organic carbon, and dissolved organic nitrogen, making rational inferences about the unobserved initial conditions at the time of eddy formation. Results consistently suggest that NCP in the center of the eddy was substantially enhanced relative to the surrounding waters, ranging from 14.1 ± 10.6 (0–110 m: within the euphotic zone) to 14.2 ± 9.2 (0–50 m: within the mixed layer) to 18.5 ± 10.7 (0–75 m: within the deep chlorophyll-maximum layer) $\text{mmol C m}^{-2} \text{d}^{-1}$ depending on the depth of integration. NCP in the ambient waters outside the eddy averaged about 2.37 ± 4.24 $\text{mmol C m}^{-2} \text{d}^{-1}$ in the mixed layer (~0–95 m). Most of the enhanced NCP inside the eddy appears to have accumulated as dissolved organic carbon (DOC) rather than exported as particulate organic carbon (POC) to the mesopelagic. Our results also suggest that the upper euphotic zone (0–75 m) above the deep chlorophyll maximum is characterized by positive NCP, while NCP in the lower layer (>75 m) is close to zero or negative.

© 2008 Elsevier Ltd. All rights reserved.

1. Introduction

In the subtropical open ocean, both production and community structure are controlled to a large extent by the limited availability of macro and trace nutrients. As a result, much of the primary production (PP) in these systems uses recycled nutrients (i.e. regenerated production), and is dominated by a microbial food web (Dugdale and Goering, 1967). New production (NP) is by definition the portion of PP sustained by exogenous nutrients. At steady state, it is often equated with net community production (NCP, defined as net autotrophic production minus community respiration, theoretically $\text{NCP} \leq \text{NP}$) and to be balanced by the sinking of organic matter from the euphotic zone (Platt et al., 1989; Williams, 1993; Allen et al., 1996; McGillicuddy and Robinson, 1997; Williams and Follows, 1998). Within the oligotrophic subtropical ocean, however, basin-wide geochemical

estimates of NP are substantially higher than that which can be explained by direct biological and physical estimates of PP and nutrient supply (Shulenberg and Reid, 1981; Jenkins and Goldman, 1985). As such, nitrogen fixation by cyanobacteria and episodic nutrient injections by mesoscale eddies and submesoscale processes, events easily missed by traditional sampling methods, have been invoked to explain the discrepancy (Falkowski et al., 1991; Capone et al., 1997; McGillicuddy and Robinson, 1997; McGillicuddy et al., 1998; Siegel et al., 1999).

Eddies are ubiquitous features throughout the oceans, with observations ranging from the Gulf of Alaska (Crawford and Whitney, 1999) to the Arabian Sea (Dickey et al., 1998; Honjo et al., 1999; Fischer et al., 2002). Although few in number, studies of eddy biogeochemistry have shown that eddy-induced local upwelling of new nutrients (e.g., nitrogen) into the euphotic zone, increases PP and NCP, influences plankton community structure, and enhances particle export to the mesopelagic (Falkowski et al., 1991; Olaizola et al., 1993; Allen et al., 1996; Anderson et al., 1996; McGillicuddy et al., 1998, 2003, 2007; Siegel et al., 1999; Seki et al., 2001; Bidigare et al., 2003; Vaillancourt et al.,

* Corresponding author. Tel.: +1 706 542 1285; fax: +1 706 542 5888.

E-mail address: wcai@uga.edu (W.-J. Cai).

2003; Benitez-Nelson et al., 2007). Yet, the global biogeochemical significance of eddies remains enigmatic and controversial (e.g., Oschlies and Garcon, 1998; McGillicuddy et al., 1998; Oschlies, 2002). Current estimates suggest that 10–50% of annual PP is due to eddy-induced nutrient fluxes (Falkowski et al., 1991; McGillicuddy et al., 1998; Oschlies and Garcon, 1998; Siegel et al., 1999; Letelier et al., 2000). This wide range reflects a paucity of direct observations of the biological and biogeochemical impacts of eddies, along with difficulties in placing the existing observations into a broader context (Haury, 1984; McNeil et al., 1999; Savidge and Williams, 2001; Bidigare et al., 2003).

The overall effect of episodic eddies on inorganic carbon cycling also remains vague. Williams and Follows (1998) argued that the eddy-pumping mechanism, i.e. eddy-mediated upwelling of nutrient-replete deep water into otherwise oligotrophic surface waters (Falkowski et al., 1991; McGillicuddy et al., 1998; Oschlies, 2002), does not necessarily lead to a corresponding decrease in dissolved inorganic carbon (DIC). Rather, they suggested that increased DIC consumption due to photosynthesis is balanced or even surpassed by the upwelling of DIC-rich waters from below. The biogeochemical evolution of the carbon dioxide system was examined in long-lived anticyclonic Haida eddies in the subpolar gyre of the North Pacific Ocean (Chierici et al., 2005). Dramatic seasonal changes in DIC and nutrients inside Haida eddies (with DIC losses during spring and gains during fall) highlight the importance of sporadic events and their complicated influence on the regional oceanic inorganic carbon biogeochemistry, although Haida eddies occur in the subpolar gyre and are physically different from subtropical mesoscale eddies (e.g., formation mechanism and maintenance, scale and duration).

The E-Flux Program was a multidisciplinary effort to understand the physical, chemical and biological characteristics of subtropical cyclonic eddies that form in the lee of main Hawaiian Islands (Benitez-Nelson et al., 2007; Dickey et al., 2008). In this region, island topography and prevailing northeasterly trade winds combine to generate mesoscale eddies in the 'Alenuihaha Channel between the islands of Maui and Hawaii. They are formed at all times of the year (mean generation frequency = 60 d), but most frequently during periods of high trade wind activity (late summer through winter). Spanning an average diameter of 180 km, these ephemeral features have typical life spans of 2–8 months (Patzert, 1969; Lumpkin, 1998; Chavanne et al., 2002; Dickey et al., 2008). This area thus serves as an ideal natural laboratory, providing excellent opportunities for examining eddy biogeochemistry at various stages of eddy development and decay (Falkowski et al., 1991; Seki et al., 2001; Bidigare et al., 2003; Vaillancourt et al., 2003). In this study, we examined NCP and inorganic carbon biogeochemistry in a first baroclinic-mode cyclonic eddy, subsequently named Cyclone *Opal*, during the third cruise of the E-Flux Program (E-Flux III). Data from an earlier cruise (E-Flux II) prior to eddy formation are also used to assess hydrographic changes through time and to make inferences about initial conditions.

2. Methods

2.1. Description of Cyclone *Opal* and sampling strategy

Cyclone *Opal* first appeared in sea-surface temperature (SST) imagery obtained from Geostationary Operational Environmental Satellite (GOES) to the southwest of the Alenuihaha Channel between February 18 and 25, 2005, as a result of strong and persistent trade winds in early February (Fig. 1A) (Benitez-Nelson et al., 2007; Dickey et al., 2008). Sampling occurred during the E-Flux III field experiment from March 10 to 28, 2005 aboard the

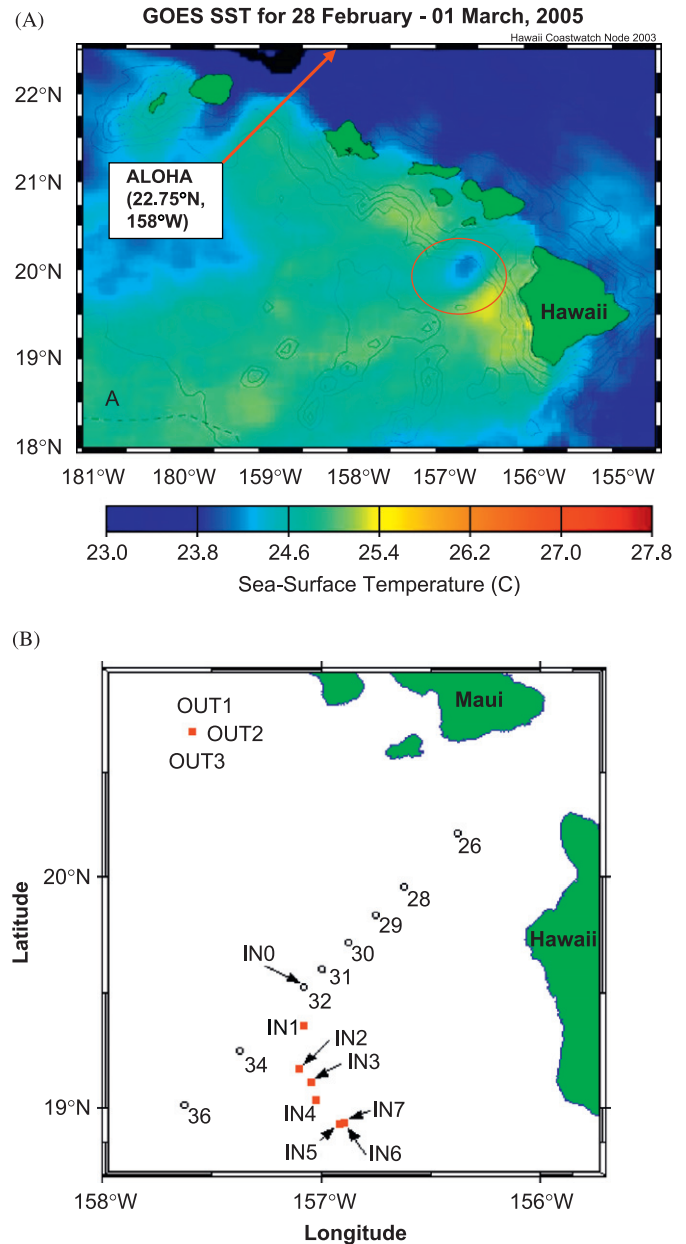


Fig. 1. Area map for the E-Flux III cruise in March 2005 in the lee of Hawaii: (A) remote sensing of GOES SST image, red circle highlights the cold core of Cyclone *Opal*, and (B) location of sampling stations, including Transect 3 stations, IN-stations, and OUT-stations. Detail information is available in Table 1.

R/V *Wecoma*, approximately 4–6 weeks after *Opal*'s first appearance. During the first week of sample collection (March 10–15), a series of five ~180-km-long transects were conducted across the eddy center to define Cyclone *Opal*'s physical and initial biological characteristics (Dickey et al., 2008; Nencioli et al., 2008). Transects 1, 2, 4, and 5 were characterized by repeat CTD casts. Transect 3 was intensively sampled for a suite of biological parameters including nutrients and carbon parameters (see Section 2.2). Results suggested that *Opal*'s diameter was ~160–180 km wide and circular in shape (Nencioli et al., 2008). A deep chlorophyll maximum layer (DCML) occurred between the $\sigma_t = 24.2$ and 24.4 kg m^{-3} isopycnal surfaces (Rii et al., 2008), shoaling from 110 m at the eddy edge to 70–90 m at the eddy center with >2-fold increase in chlorophyll concentrations (Rii et al., 2008). These preliminary measurements suggested that

Cyclone *Opal* was in a physically and biologically mature phase of eddy development (Sweeney et al., 2003).

A 7-day time-series of process studies were then conducted at the eddy center (IN-stations) from March 16 to 22 to describe the temporal biogeochemical evolution of Cyclone *Opal* during the course of a decaying diatom bloom (Benitez-Nelson et al., 2007). During this period, Cyclone *Opal* moved rapidly to the south (average translational speed of 0.33 km h^{-1}) by $\sim 160 \text{ km}$ from its initial location (e.g., traveled from IN1 to IN7, Table 1 and Fig. 1B) (Nencioli et al., 2008). Acoustic Doppler current profiler (ADCP) data, SST, and satellite observations were used to evaluate if each hydrographic cast was positioned close enough to the eddy center (velocity $\leq 25 \text{ cm s}^{-1}$ as a threshold value) to be considered as an IN-station (Nencioli et al., 2008). As a result, nine out of the 51 CTD casts were excluded, including cast 49 (i.e., IN1 in Table 1 and Fig. 1B). Once completed, a series of three control stations (OUT-stations) were sampled during March 24–27 at a location well removed from the eddy flow field ($>200 \text{ km}$ north of IN7, Fig. 1B), but still within the lee of the Hawaiian Islands (Dickey et al., 2008).

Approximately 6 weeks prior to E-Flux III, the E-Flux II field campaign was conducted during January 10–28, 2005 aboard the R/V *Wecoma*. No mesoscale eddies were observed due to the lack of northeasterly trade winds during the sampling period (Dickey et al., 2008). Thus, the data from this cruise, considered to be some what representative of the initial waters from which Cyclone *Opal* is derived, are used for comparison purposes with E-Flux III as needed and for making inferences about initial conditions.

2.2. Sample collection and analyses

Discrete water samples were collected over the upper 350 m for pH, total alkalinity (TAlk), DIC, inorganic nutrients (including nitrate and nitrite (N+N)), total organic carbon (TOC), and dissolved organic nitrogen (DON) using a SeaBird SBE 9/11+CTD system with rosette sampler (Table 1 and Fig. 1B). Samples were collected during Transect 3 (stations 26–36 in Fig. 1B) and each

IN- and OUT-station (equivalent to once per day) (Table 1 and Fig. 1B). A large range of additional measurements were also conducted by other researchers (e.g., Benitez-Nelson et al., 2007; Dickey et al., 2008; Rii et al., 2008). Here, only the hydrographic data and biogeochemical parameters related to this paper are described.

Inorganic carbon parameters were measured using standard protocols. pH was measured at a constant temperature (25°C) with a Ross combination glass pH electrode (Orion Research). The calibration was conducted by using three NBS pH buffers (pH = 4, 7, 10) to calculate its response slope and a tris buffer at salinity 35 to derive a seawater pH scale. The accuracy was ± 0.01 pH units. TAlk was determined by Gran titration using 0.1 M HCl on board ship (Cai and Wang, 1998; Wang and Cai, 2004). The titration was calibrated with a certified reference material (CRM) from A.G. Dickson. Under constant temperature condition (25°C), the precision and accuracy of the titration were 0.1%. On shipboard condition, the fluctuation of laboratory temperature (1°C or more) resulted in these values to be 0.3% or $\pm 7 \mu\text{mol kg}^{-1}$. Water samples for DIC analysis were collected in 20-ml vials and preserved with $10 \mu\text{l}$ saturated mercuric chloride. The samples were stored refrigerated prior to analysis (Cai and Wang, 1998; Wang and Cai, 2004). Based on replicate analysis, DIC precision was determined to be within $\pm 2 \mu\text{mol kg}^{-1}$. The accuracy of the analysis is assured by the calibration against the CRM. $p\text{CO}_2$ in Fig. 2H was calculated (to within $\pm 10\text{--}15 \mu\text{atm}$ of the underway $p\text{CO}_2$ data) from measured pH and DIC data under 25°C and 1-atm conditions by using the carbonic acid dissociation constants of Mehrbach et al. (1973) as refitted by Dickson and Millero (1987) (Mehrbach et al., 1973; Dickson and Millero, 1987). Underway sea-surface $p\text{CO}_2$ measurements were conducted along all transects and at process stations. Estimates of CO_2 air-sea fluxes are described in detail by Chen et al. (2007).

Water samples for inorganic nutrients (including N+N) and DON were frozen immediately and stored frozen at $\sim -20^\circ\text{C}$ until analysis (see Rii et al. (2008) and Mahaffey et al. (2008), for more detail). Samples for inorganic nitrogen were analyzed by Joe Jennings at Oregon State University using a continuous segmented flow system consisting of components of both a Technicon

Table 1
Stations and casts information for E-Flux III cruise

Station no.	Longitude ($^\circ\text{W}$)	Latitude ($^\circ\text{N}$)	Sampling time	Cast no. (DIC)	Cast no. (NUTS)	Cast no. (TOC/DON)
<i>Sampled transect</i>						
26	156.22.40	20.11.32	3/13/2005	13	13	N/A
28	156.37.46	19.57.22	3/13/2005	15	15	N/A
29	156.44.98	19.50.14	3/13/2005	16	16	N/A
30	156.52.47	19.43.04	3/13/2005	17	17	N/A
31	156.59.98	19.36.00	3/13/2005	18	18	N/A
32	157.4.92	19.31.38	3/13/2005	19a	19a	N/A
34	157.22.46	19.14.78	3/13/2005	23	23	N/A
36	157.37.44	19.00.70	3/13/2005	25	25	N/A
<i>IN-stations and OUT-stations</i>						
INO ^a	157.4.92	19.31.38	3/13/2005	19a	19a	N/A
IN1 ^b	157.4.77	19.21.37	3/16/2005	49	N/A	N/A
IN2	157.6.00	19.10.00	3/17/2005	63	63	59
IN3	157.02.70	19.06.70	3/18/2005	67	67	67
IN4	157.01.53	19.01.80	3/19/2005	74	73	73
IN5	156.53.8	18.56.19	3/20/2005	86	82	82
IN6	156.51.59	18.55.78	3/21/2005	93	88	88
IN7	156.51.57	18.55.83	3/22/2005	N/A	94	94
OUT1	157.35.36	20.37.33	3/24/2005	111	111	111
OUT2	157.35.42	20.37.33	3/25/2005	119	119	119
OUT3	157.35.43	20.37.32	3/26/2005	127	127	127

^a INO is cast 19a at station 32. We call it INO since it has the characteristics of IN-stations.

^b IN1 is not considered as IN-station from velocity analysis by using ADCP data.

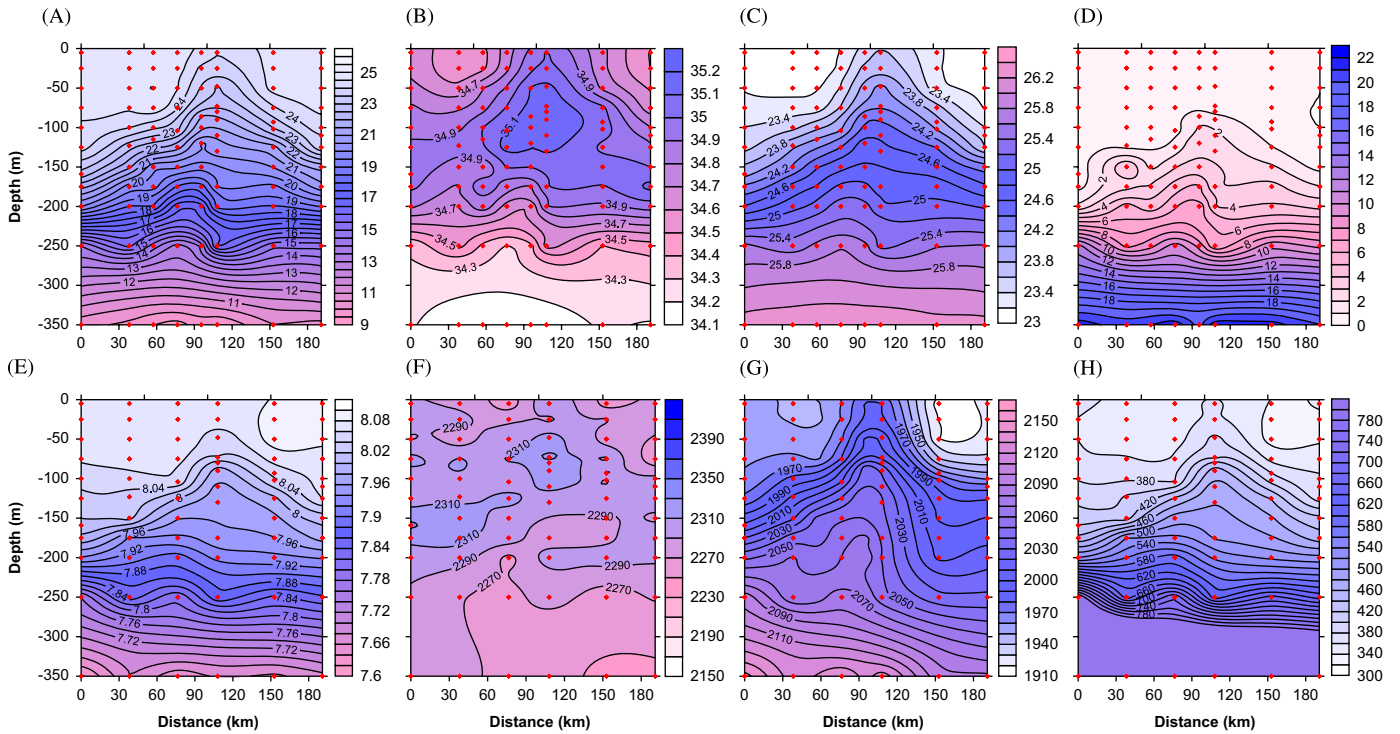


Fig. 2. Vertical sections ((A) temperature ($^{\circ}\text{C}$); (B) salinity; (C) density (σ_t); (D) N+N (μM); (E) pH; (F) TALK ($\mu\text{mol kg}^{-3}$); (G) DIC ($\mu\text{mol kg}^{-3}$); (H) $p\text{CO}_2$ (μatm) (calculated from pH and DIC, coefficients come from documents (Mehrbach et al., 1973; Dickson and Millero, 1987)) for the sampled transect from station 26 through 36 (red dots represent real data). For the horizontal axis label, station 26 is located where distance is zero, and station 36 is located on the other side. Note that temperatures were not corrected to potential temperature since the data discussed do not exceed 350 m and deviation resulted in less than 0.03°C .

Autoanalyzer IITM and an Alpkem RFA 300TM (Gordon et al., 1994). Inorganic nitrogen precision was estimated to be $0.2 \mu\text{M}$. DON was calculated as the difference between total dissolved nitrogen (TDN) and inorganic nitrogen. TDN was measured at Craig Carlson's laboratory at the University of California, Santa Barbara (Mahaffey et al., 2008). The precision for TDN and DON is $\pm 0.5 \mu\text{M}$. Samples for TOC (unfiltered water samples frozen until measurement) were analyzed via high-temperature combustion using a Shimadzu TOC-V at Carlson's laboratory as well. The operating conditions of the Shimadzu TOC-V were slightly modified from the manufacturer's model system (Carlson et al., 2004). The precision for TOC measurement is $\pm 1 \mu\text{M}$.

3. Observations

3.1. Hydrology and carbonate chemistry across Cyclone Opal

Vertical sections of Cyclone Opal from Transect 3 were characterized by intense uplift of isothermal, isohaline, and isopycnal surfaces in the upper 250 m across the 40-km eddy core (Figs. 2A–C) (Dickey et al., 2008; Nencioli et al., 2008). Differential anomalies of temperature and density were confined between 40 and 160 m depth (Nencioli et al., 2008). In contrast, salinity had a subsurface maxima within the eddy core characterized by a positive salinity differential anomaly (~ 0.2) above a region of high negative salinity differential anomaly (about -0.4) (Fig. 2B) (Nencioli et al., 2008).

Vertical sections of carbonate parameters (Figs. 2E, G, and H) and N+N (Fig. 2D) all showed substantial vertical displacements across the eddy center. For example, DIC concentrations of $1990 \mu\text{mol kg}^{-1}$ shoaled from 130–160 m at the eddy edge to 40–60 m at the eddy center, following the $\sigma_t = 24 \text{ kg m}^{-3}$ isopycnal surface (Fig. 2C and Nencioli et al. (2008)). Hydro-

graphic data (Figs. 2A–C), DIC (Fig. 2G), and calculated $p\text{CO}_2$ (Fig. 2H) all suggest an intrusion of cold, salty, DIC-rich deep water into the upper water that outcropped at the surface at the eddy center. In contrast, although isopleth uplift also occurred at the eddy center, no significant increase in N+N or decrease in pH in the upper 50 m was observed (Figs. 2D and E). The same conclusions can be derived from corresponding depth profiles of the above properties (Fig. 3).

The lack of a substantial concentration increase in N+N (or positive N+N anomalies) in the upper 50 m at the eddy core is likely due to the enhanced biological consumption there (see Section 3.2). This enhanced biological production also serves to increase pH, thus partially ameliorating the influence of uplifted low pH deep water. Finally, TALK vertical section shows little variation in the upper 200 m as may be expected (Fig. 2F). Variation is within the uncertainties of the measurement, and therefore, hindered further discussion.

3.2. IN- versus OUT-stations

In order to understand the biogeochemistry of Cyclone Opal, it is first necessary to describe typical water mass distributions in the North Pacific subtropical gyre. The temperature–salinity (T – S) relationships observed throughout the study are typical for the subtropical waters surrounding Hawaii, and are similar to Station ALOHA, site of the Hawaii Ocean time-series program (HOT), located 100 km due north of Oahu (Figs. 1A and 4A) (Sabine et al., 1995; Li et al., 2000). The water column is comprised of subtropical surface water, subtropical salinity maximum water ($150 \pm 30 \text{ m}$), and shallow salinity minimum water ($320 \pm 30 \text{ m}$) (Wyrtki and Kilonsky, 1984; Sabine et al., 1995; Li et al., 2000). IN- and OUT-stations in E-Flux II and E-Flux III have similar T – S relationships in the upper water column (Fig. 4A). Depth profiles of T and S reveal how subtropical salinity maximum water was

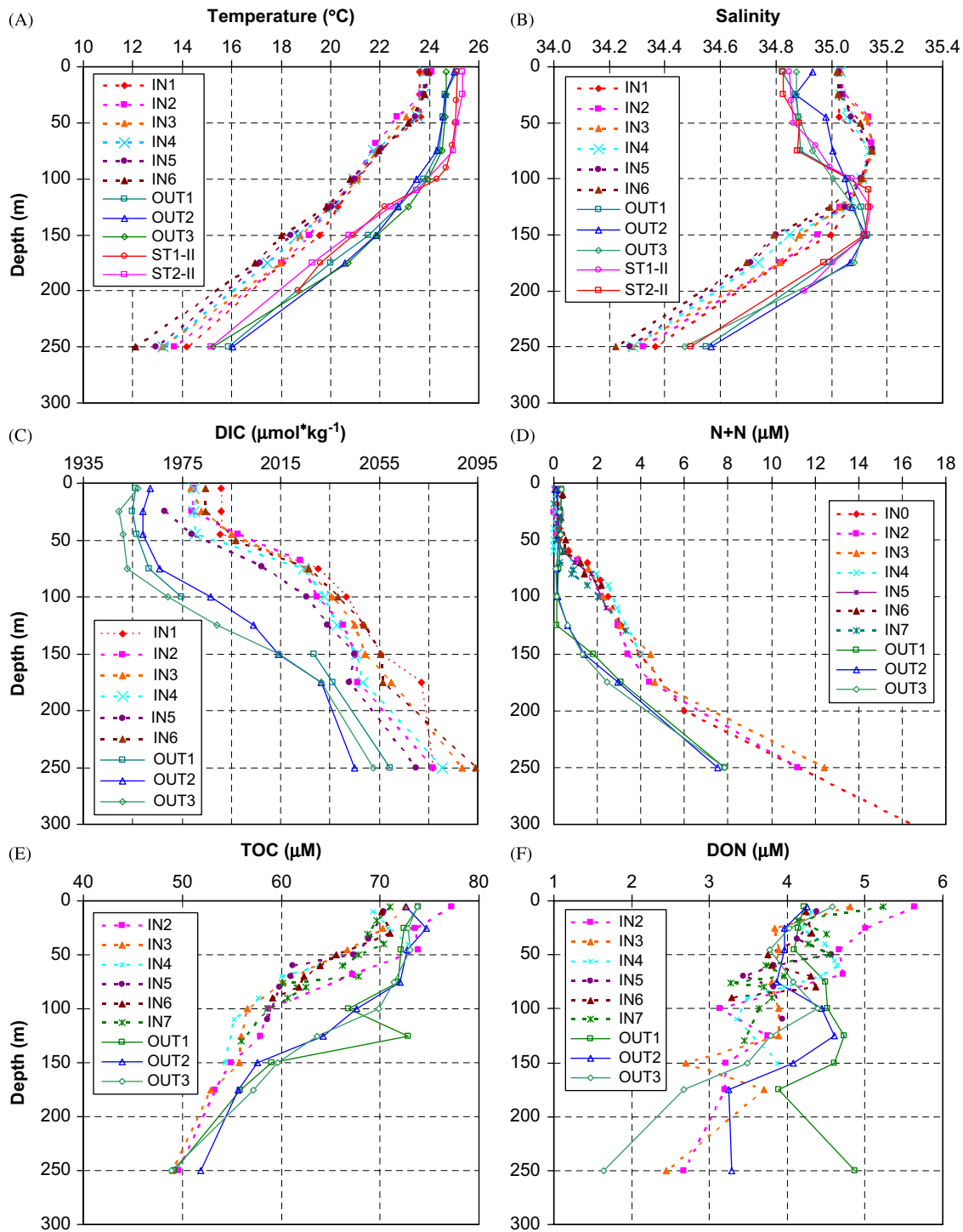


Fig. 3. Vertical profiles of (A) temperature, (B) salinity, (C) DIC, (D) nitrate+nitrite (N+N), (E) TOC, and (F) DON vs. depth at IN- and OUT-stations during E-Flux III. Please note that for (A) and (B), ST1-II and ST2-II are two stations from E-Flux II cruise in January 2005.

uplifted from 150 m at OUT-stations to ~60–90 m at IN-stations at the eddy center (Figs. 3A and B). Mixed-layer depths averaged 51 ± 8 m at IN-stations and 95 ± 7 m at OUT-stations, respectively. Here, we define the mixed-layer depth (MLD) as the depth at which seawater temperature is 1°C less than the temperature at 10 m, following the convention established by Benitez-Nelson et al. (2007) and Nencioli et al. (2008).

Surface water at the center of Cyclone *Opal* was 0.160–0.171 saltier and 1.076 – 1.817°C colder than the surrounding ocean depending on the depth of integration (Table 2 and Figs. 3A, B).

Here, the concept of ‘surface water’ generally refers to the water mass in the mixed layer, i.e., 0–50 m at the eddy center and 0–95 m in ambient waters outside the eddy. However, for the purpose of this study, in addition to the MLD, we also define two other depth horizons at the eddy center: 0–75 m (the depth of the DCML) and 0–110 m (just below the 1% light level). Cooler and saltier surface waters at IN-stations suggest that they had been influenced by the intrusion and mixing of deeper subtropical salinity maximum water from below (Figs. 3B, 4A and Table 2). Below the salinity maximum, the linear decrease in salinity

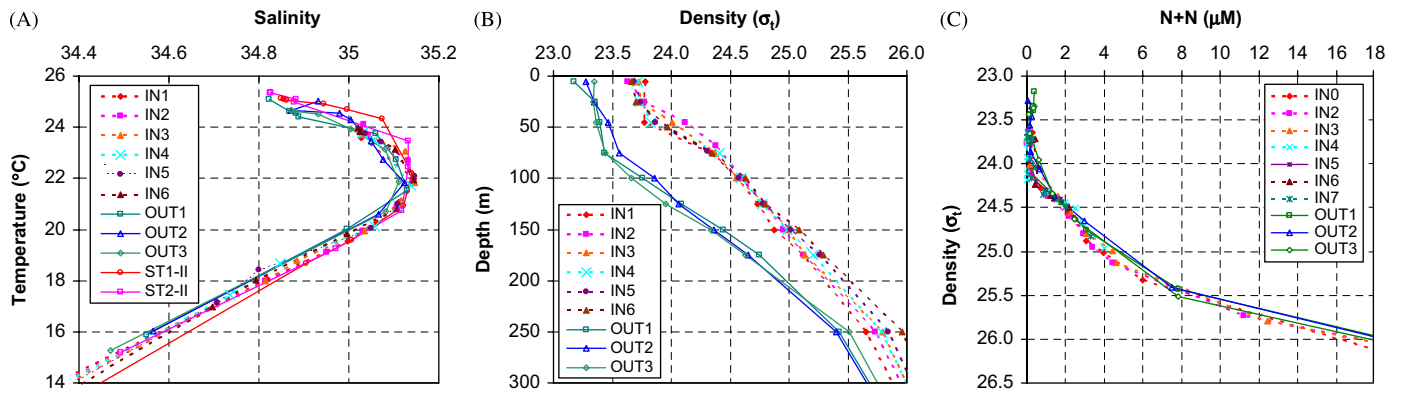


Fig. 4. (A) Diagram of salinity vs. temperature; (B) profile of density vs. depth; and (C) profile of N+N vs. density at IN-stations and OUT-stations during E-Flux III. Note that for part (A), ST1-II and ST2-II are two stations from E-Flux II cruise in January 2005.

Table 2

Average observed depth-integrated temperature and salinity over three depth horizons (0–50, 0–75, and 0–110 m) at IN- and OUT-stations during E-Flux III

Stations	Temperature _{obs} (°C)	Salinity _{obs}
IN _{avg} (0–50 m)	23.647 ± 0.056	35.044 ± 0.013
OUT _{avg} (0–50 m)	24.723 ± 0.056	34.882 ± 0.030
IN _{avg} (0–75 m)	23.234 ± 0.081	35.071 ± 0.016
OUT _{avg} (0–75 m)	24.627 ± 0.016	34.900 ± 0.041
IN _{avg} (0–110 m)	22.631 ± 0.100	35.089 ± 0.012
OUT _{avg} (0–110 m)	24.448 ± 0.057	34.929 ± 0.038
OUT _{deep} (150 m)	21.738 ± 0.179	35.122 ± 0.009

reflects mixing between the subtropical salinity maximum water and the shallow salinity minimum water (Sabine et al., 1995).

At OUT-stations, surface water salinity and temperature were 34.900 ± 0.041 and 24.627 ± 0.016 °C, respectively (Table 2). These are comparable to the 14-year mean salinity and temperature in March at Station ALOHA, 35.038 and 24.74 °C (Keeling et al., 2004). Lower salinities in the lee of Hawaii relative to station ALOHA suggest a greater intrusion of tropical surface water from lower latitudes. Average DIC and *n*DIC (salinity 35 normalized DIC) in spring 2005 were 1956.8 ± 4.4 and 1962.4 ± 4.5 $\mu\text{mol kg}^{-1}$, respectively (Table 3). At Station ALOHA, spring 2005 average *n*DIC was ~ 1984 $\mu\text{mol kg}^{-1}$, using DIC values measured in 2002 (from Keeling et al., 2004) and considering seasonal and long-term changes (DIC reaches its peak in April and *n*DIC increased on average by 1.22 ± 0.08 $\mu\text{mol kg}^{-1} \text{yr}^{-1}$, Keeling et al. (2004)). The *n*DIC at our OUT-stations was ~ 22 $\mu\text{mol kg}^{-1}$ lower than that at Station ALOHA. This difference is likely due to the influence of lower DIC surface water from the south, as suggested previously by other studies (Winn et al., 1994; Quay and Stutsman, 2003; Keeling et al., 2004).

The uplift of isopycnal surfaces at the core of Cyclone *Opal* influenced biogeochemical parameters relative to surrounding waters (Figs. 3C–F), a conclusion further supported by the close relationship between N+N concentration and density at both IN- and OUT-stations (e.g., Fig. 4C). These uplifted deeper waters were generally rich in nutrients and DIC, but poor in total and dissolved organic matter (Figs. 3C–F) (Benitez-Nelson et al., 2007). Mixed layer DIC at IN-stations averaged 1983.8 ± 3.2 $\mu\text{mol kg}^{-1}$ and *n*DIC 1986.3 ± 3.3 $\mu\text{mol kg}^{-1}$ (Table 5, $\mu\text{M} \cdot 1.1241 \text{ kg dm}^{-3}$ (density) = $\mu\text{mol kg}^{-1}$). Surface water DIC at the eddy center was therefore ~ 25 $\mu\text{mol kg}^{-1}$ higher than surrounding waters at OUT-stations. This difference is comparable to the seasonal variability (± 15 $\mu\text{mol kg}^{-1}$) at Station ALOHA (Keeling et al., 2004). In contrast, TOC was much lower than that at OUT-stations at every depth horizon. There was no obvious difference in DON

between IN- and OUT-stations, mainly due to substantially lower DON concentrations and larger relative uncertainties.

Unlike TOC and DIC, N+N concentrations within the MLD at IN-stations (Fig. 3D) were the same, within error, as that observed at OUT-stations and also were similar to those found from Transect 3 (see Section 3.1). The lack of a substantial concentration increase (or positive N+N anomalies, Nencioli et al. (2008)) in the mixed layer could have been a result of rapid biological consumption immediately after the initial eddy-pumping event (Rii et al., 2008). This is further evident by the much shallower layer of available N+N and sharper nutricline at IN-stations (Figs. 3D and 4B). This conclusion is also supported by enhanced growth and production rates of the *Prochlorococcus* spp.-dominated ambient community at IN-stations, although there is little compositional or biomass response in the mixed layer (Landry et al., 2008).

4. Mass balance models for NCP estimation

The hydrological characteristics and physical processes at OUT- and IN-stations were very different. OUT-stations were dominated by mixing across a stable pycnocline, whereas IN-stations were influenced by the doming of isopycnal surfaces across the eddy feature. Thus, different mass balance models are required for estimating NCP.

4.1. Mixed layer model for NCP estimation at OUT-stations

The mass balance approach used in the mixed layer outside the eddy is a classical approach in the subtropical open ocean. The mixed-layer DIC budget typically incorporates the following processes: (1) air–sea gas exchange, (2) vertical diffusion from below, (3) entrainment of DIC from the thermocline during mixed-layer deepening, (4) horizontal transport, and (5) NCP (Gruber et al., 1998; Lee, 2001; Quay and Stutsman, 2003; Keeling et al., 2004). Here, we apply this model to OUT-stations using the following general equation and solving for NCP:

$$\frac{d\text{DIC}_{\text{Inventory}}}{dt} = F_{\text{air-sea}} + F_{\text{Diff}} + F_{\text{Adv}} + F_{\text{Entrain}} - \text{NCP}_{\text{DIC}} \quad (1)$$

where NCP is NCP in the mixed layer, $d\text{DIC}_{\text{Inventory}}/dt$ is the change in DIC inventory in the mixed layer over time, and $F_{\text{air-sea}}$ is the air to sea CO_2 flux at the surface with the direction from air to sea, which averaged 2.9 ± 1.8 $\text{mmol C m}^{-2} \text{day}^{-1}$ outside Cyclone *Opal* during E-Flux III (Chen et al., 2007). F_{Diff} for DIC is the vertical diffusive flux of DIC from below and is estimated from the vertical diffusion coefficient (K_z) and vertical gradient of DIC versus depth

Table 3
Average observed concentrations over three depth horizons (0–50, 0–75, and 0–110 m) at OUT-stations during E-Flux II and E-Flux III cruises

	DIC ($\mu\text{mol kg}^{-1}$)		Salinity		N+N (μM)		TOC (μM)		DON (μM)	
	E-Flux II (n = 8)	E-Flux III (n = 3)	E-Flux II (n = 6)	E-Flux III (n = 3)	E-Flux II (n = 6)	E-Flux III (n = 3)	E-Flux II (n = 6)	E-Flux III (n = 3)	E-Flux II (n = 6)	E-Flux III (n = 3)
OUT _{avg} (0–50 m)	1950.3 ± 5.1	1956.0 ± 3.2	34.858 ± 0.015	34.882 ± 0.030	0.04 ± 0.03	0.28 ± 0.08	72.40 ± 0.42	73.19 ± 0.38	4.56 ± 0.34	4.11 ± 0.05
OUT _{avg} (0–75 m)	1952.0 ± 5.7	1956.8 ± 4.4	34.875 ± 0.024	34.900 ± 0.041	0.04 ± 0.03	0.25 ± 0.07	72.08 ± 0.79	72.80 ± 0.28	4.51 ± 0.32	4.09 ± 0.11
OUT _{avg} (0–110 m)	1960.9 ± 6.3	1960.6 ± 3.4	34.926 ± 0.026	34.929 ± 0.038	0.13 ± 0.07	0.22 ± 0.05	70.35 ± 0.78	71.88 ± 0.35	4.45 ± 0.33	4.16 ± 0.13
OUT _{deep}	2025.3 ± 4.8	2019.4 ± 3.2	35.131 ± 0.010	35.122 ± 0.009	1.85 ± 0.33	1.51 ± 0.26	59.17 ± 1.64	58.74 ± 1.01	3.91 ± 0.39	3.78 ± 0.56

OUT_{deep} represents the subtropical salinity maximum water between 125 and 150 m at OUT-stations. E-Flux II data in this table were collected between January 16 and 26, 2005. E-Flux III data were collected between March 24 and 26, 2005.

below the mixed layer. F_{Adv} is the DIC flux from horizontal and vertical advection and is calculated from the horizontal or vertical velocity and the DIC gradient. Advection is assumed to be zero for OUT-stations. The uncertainty introduced by this assumption is discussed in Section 5.1. F_{entrain} is the entrainment flux of DIC from the thermocline whenever the mixed-layer deepens, and is also assumed to be zero since the MLD at OUT-stations during E-Flux II (January 10–28, 2005) and E-Flux III (March 10–28, 2005) was, within error, identical (Dickey et al., 2008). All flux units are in $\text{mmol C m}^{-2} \text{day}^{-1}$. Steady state ($dC_{\text{inventory}}/dt = 0$) is assumed since DIC as well as salinity, N+N, TOC, and DON between E-Flux II and III at OUT-stations showed little variability in the upper water column (Table 3) (see Section 5.1). Thus, this mixed-layer model is only applied to the winter season.

Similar mass balance equations can be written to estimate NCP from N+N, TOC, and DON. For example, the mass balance for “new nitrogen” (N+N) is described by the following equation (note the absence of the air–sea gas exchange term):

$$\text{NCP}_{\text{N+N}} = \left(F_{\text{Diff}} + F_{\text{Adv}} - \frac{d(\text{N+N})_{\text{Inventory}}}{dt} \right) \times (\text{C/N})_{\text{DOM}} \quad (2)$$

where $d(\text{N+N})_{\text{Inventory}}/dt$ is the change of N+N over time in the mixed layer, the Redfield ratio of carbon (C) to nitrogen (N) in organic matter ($(\text{C/N})_{\text{DOM}}$) is ~ 6.6 (Redfield, 1958). For the mass balance equation of TOC, an additional term, F_{Export} , must be added, which represents the particulate organic carbon (POC) flux exported out of a defined layer (averaged $1.25 \pm 0.51 \text{ mmol C m}^{-2} \text{day}^{-1}$ at 150 m at OUT-stations using sediment traps and ^{234}Th -derived fluxes (Benitez-Nelson et al., 2007)):

$$\text{NCP}_{\text{TOC}} = \frac{d\text{TOC}_{\text{Inventory}}}{dt} + F_{\text{Export}} - F_{\text{Diff}} - F_{\text{Adv}} \quad (3)$$

where $d\text{TOC}_{\text{Inventory}}/dt$ is the change of TOC over time in the mixed layer. For TOC, suspended and sinking particles are a minor component ($\leq 5\%$), such that it is mainly comprised of dissolved organic carbon (DOC) (Landry et al., 2008; Mahaffey et al., 2008). Thus, the diffusive flux (F_{Diff}) can still be estimated by K_z and a vertical gradient. The DON mass balance does not include a particle flux term since we only consider the dissolved phase:

$$\text{NCP}_{\text{DON}} = \left(\frac{d\text{DON}_{\text{Inventory}}}{dt} - F_{\text{Diff}} - F_{\text{Adv}} \right) \times (\text{C/N})_{\text{DOM}} \quad (4)$$

where $d\text{DON}_{\text{Inventory}}/dt$ is the change of DON over time in the mixed layer. Note that DON is converted to C units using a C:N ratio for dissolved organic matter (~ 13.6 , $(\text{C/N})_{\text{DOM}}$) (Benner et al., 1992).

The vertical diffusion coefficient, K_z , was determined according to (Denman and Gargett, 1983):

$$K_z = 0.25 \times \varepsilon_d * N^{-2} \quad (5)$$

where ε_d denotes the rate of turbulent energy dissipation and N is the Brunt Väisälä frequency, computed from the vertical density gradient below the mixed layer (Denman and Gargett, 1983). Turbulent energy dissipation may range between 10^{-9} and $10^{-7} \text{ m}^2 \text{s}^{-3}$; here we use $2 \times 10^{-8} \text{ m}^2 \text{s}^{-3}$ as representative of the upper ocean thermocline at times of low wind speeds (Gruber et al., 1998; Quay and Stutsman, 2003). This value was applied by Gruber et al. (1998) for the seasonal inorganic carbon budget at the BATS site in the northwestern Sargasso Sea and was also used to determine K_z between 1994 and 1999 at Station ALOHA by Quay and Stutsman (2003). Using Eq. (5), we calculated a K_z of $0.3\text{--}0.5$ (or $0.42 \pm 0.05 \text{ cm}^2 \text{s}^{-1}$) for the OUT stations, which is within the range of that determined at Station ALOHA, where K_z ranged from $> 1 \text{ cm}^2 \text{s}^{-1}$ during the winter to a minimum of $\sim 0.2 \text{ cm}^2 \text{s}^{-1}$ in late summer (Quay and Stutsman, 2003). We should note that uncertainties in the K_z are typically $\pm 100\%$ or greater (Quay and Stutsman, 2003).

4.2. Two end-member mixing model for eddy-induced NCP at IN-station

Due to the uplift of deep subtropical salinity maximum water at IN-stations (Fig. 3B), our assumptions of steady state and no vertical advection used in the mixed-layer model for the OUT-stations (see Section 4.1) are likely invalid. As such, a mass balance approach based on a two end-member mixing model is used to determine the average NCP rate over the time period between Cyclone *Opal*'s formation and sample collection. Due to sampling constraints, we have no direct measurement of nutrient and other biogeochemical parameters at the exact time of eddy formation. We would expect that by the time of sampling, a significant fraction of the nutrients and DIC upwelled into surface waters had already been consumed and organic matter accumulated due to biological activity. Thus, an estimate of the initial conditions following isopycnal uplift is necessary to determine the magnitude of biologically active components consumed or produced by the biological community.

We emphasize that it is not appropriate to make direct comparisons of chemical constituents between IN- and OUT-stations since OUT-stations do not represent the initial conditions at the eddy center, i.e. the chemical composition of the water immediately following uplift, but prior to the start of biological activity. The fact that cooler and saltier surface water at IN-stations is located near the T - S line between the two water masses, the subtropical surface water and subtropical salinity maximum water (Fig. 4A), suggests that the surface water in the center of the eddy can be interpreted as a mixture of two end members. This assumption is further supported by the fact that a portion of Cyclone *Opal*, about 50 km in diameter and up to 70 m deep located at the eddy center, is isolated from the surrounding waters (well within the solid body rotation) (Nencioli et al., 2008).

Use of a two end-member mixing strategy is not unique. The theory of two end-member mixing and its use in estuarine mixing is discussed in detail by Officer (1980). Although specific physical mechanisms are not explicitly described during two end-member mixing, net results of open-ocean vertical advection and mixing are quantitatively incorporated by using a salt budget. Li et al. (2000) applied this method to water-column remineralization at Station ALOHA, and similar models based on salt budget have been applied to a range of upwelling regimes, e.g., Costa Rica Dome in the Eastern Tropical Pacific Ocean, Peru current, NW Africa, and the SW Africa upwelling systems (Broenkow, 1965; Minas et al., 1986).

In applying the two end-member mixing model, we choose salinity as the conservative tracer. It should be noted that temperature is not strictly conservative in the upper ocean due to heat exchange, and there are changes in overall heat content between E-Flux II and E-Flux III OUT stations that cannot be explained by air–sea interaction (Fig. 3A). During our cruises, SST cooled by ~0.5 °C from late January (E-Flux II) to mid-March (OUT stations in E-Flux III) (Fig. 3A). The concave upward shape of the *T–S* diagram in the upper water column, on the other hand, indicates warming of the eddy surface water (Fig. 4A). Salinity, however, remained relatively constant from January to March (Fig. 3B). We thus assume that there is no change in salinity and DIC outside the eddy during this period. We will discuss the uncertainties introduced by this simplification in Section 5.2.1.

Here, it is assumed that the surface water within the core of Cyclone *Opal* (with salinity S_{IN}) is a mixture of the deep subtropical salinity maximum water (with salinity S_d) and the original surface water, i.e. surface water at OUT-stations (with salinity S_{OUT}). The fraction of each water type in the mixture is a direct function of salinity. Therefore a salt budget model can be formulated as

$$S_{IN} = f \cdot S_d + (1 - f) \cdot S_{OUT} \quad (6)$$

with

$$f = (S_{IN} - S_{OUT}) / (S_d - S_{OUT})$$

and

$$1 - f = (S_d - S_{IN}) / (S_d - S_{OUT}) \quad (7)$$

where f is the fraction of deep salinity maximum water and $(1-f)$ is the fraction of the original surface waters. To convert this fraction to volume, we use:

$$S_{IN} \cdot V_T = V_d \cdot S_d + V_s \cdot S_{OUT} \quad (8)$$

where V_T is the total volume, $V_d = V_T \cdot f$, the volume of deep water in the mixture, and $V_s = V_T \cdot (1-f)$, the volume of surface water in the mixture (Fig. 5).

Thus, the expected initial DIC concentration ($DIC_{IN(exp)}$) in the center of the eddy due to two end-member mixing in the absence of biological process can be determined as

$$DIC_{IN(exp)} = (V_d \cdot DIC_d + V_s \cdot DIC_{OUT}) / V_T \quad (9)$$

or,

$$\begin{aligned} DIC_{IN(exp)} &= f \cdot DIC_d + (1 - f) \cdot DIC_{OUT} \\ &= DIC_d \cdot \frac{(S_{IN} - S_{OUT})}{(S_d - S_{OUT})} \\ &\quad + DIC_{OUT} \cdot \frac{(S_d - S_{IN})}{(S_d - S_{OUT})} \end{aligned} \quad (10)$$

where the subscripts of DIC_{OUT} and DIC_d describe the concentrations of DIC measured in OUT-station surface water with salinity S_{IN} and in deep salinity maximum water with salinity S_d , respectively (also see explanation to Eq. (7)). Similarly, the expected initial concentrations of other desired biogeochemical parameters, such as N+N, TOC, and DON, in the IN-station surface waters can also be calculated as a function of salinity.

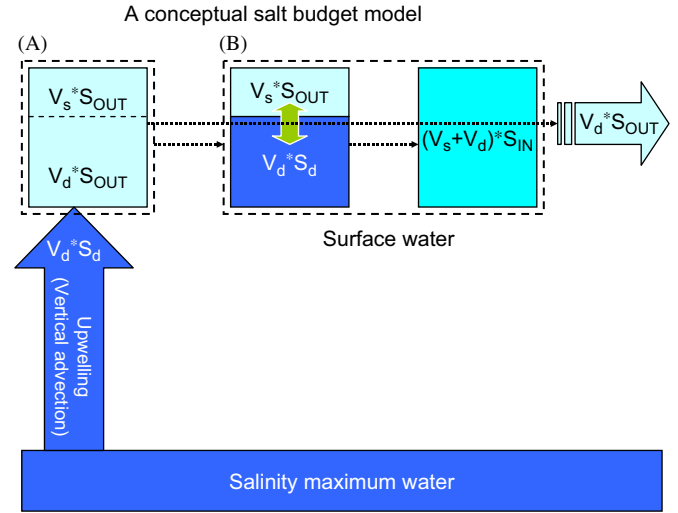


Fig. 5. Conceptual salt budget model for the eddy case: (A) before subsurface salinity maximum water intruding the surface layer inventory; and (B) after the eddy-induced intrusion of salinity maximum deep water in the surface layer inventory. There are two balances here: (1) water mass balance: $V_T = V_s + V_d$; and (2) salt mass balance: $V_s S_{OUT} + V_d S_d = (V_s + V_d) S_{IN}$.

Let us now examine the meaning of $DIC_{IN(exp)}$ further. The change in DIC inventory in a surface layer over the course of eddy development can be represented by the following mass balance equation:

$$\frac{dDIC_{Inventory}}{dt} = \sum DIC_{Input} - \sum DIC_{Output} + F_{air-sea} - NCP_{DIC} \quad (11)$$

where DIC_{input} and DIC_{output} are the total input and output rate of DIC, respectively. $F_{air-sea}$ is the average flux of CO_2 air–sea exchange at the eddy center. During E-Flux III, this flux was estimated to be $2.4 (\pm 1.8) \text{ mmol C m}^{-2} \text{ day}^{-1}$ (with the direction from air to sea) (Chen et al., 2007). Applying the same salt budget model concept to DIC (Fig. 5), we have,

$$\frac{dDIC_{Inventory}}{dt} = V_T \cdot (DIC_{IN(obs)} - DIC_{OUT}) \cdot \frac{H}{V_T \cdot T} \quad (12)$$

and

$$\begin{aligned} \sum DIC_{Input} - \sum DIC_{Output} \\ = V_d \cdot (DIC_d - DIC_{OUT}) \cdot \frac{H}{V_T \cdot T} \end{aligned} \quad (13)$$

where H is the height of the relevant surface water column in the center of the eddy, and T is the elapsed time, i.e., time period between Cyclone *Opal's* formation and sample collection, approximately 35 days (average ~5 weeks) (Dickey et al., 2008). $DIC_{IN(obs)}$ is the observed (i.e. measured) average DIC in IN-station surface water column. By dividing all DIC inventory terms with area (H/V_T) and time (T), the unit for NCP becomes $\text{mmol C m}^{-2} \text{ d}^{-1}$. This is the unit for all the fluxes and inventory change terms in this paper.

Inserting Eqs. (12) and (13) into Eq. (11), we obtain

$$\begin{aligned} NCP_{DIC} &= \sum DIC_{Input} - \sum DIC_{Output} \\ &\quad - \frac{dDIC_{Inventory}}{dt} + F_{air-sea} \\ &= \{V_d \cdot (DIC_d - DIC_{OUT}) \\ &\quad - V_T \cdot (DIC_{IN(obs)} - DIC_{OUT})\} \\ &\quad \times \frac{H}{V_T \cdot T} + F_{air-sea} \\ &= \{V_d \cdot DIC_d + (V_T - V_d) \cdot DIC_{OUT} \end{aligned}$$

$$\begin{aligned}
 & -V_T * DIC_{IN(obs)} * \frac{H}{V_T * T} + F_{air-sea} \\
 = & \{ [V_d * DIC_d + V_s * DIC_{OUT}] / V_T \\
 & - DIC_{IN(obs)} * \frac{H}{T} + F_{air-sea}
 \end{aligned}$$

By comparing with Eq. (9), we have

$$NCP_{DIC} = (DIC_{IN(exp)} - DIC_{IN(obs)}) * \frac{H}{T} + F_{air-sea} \quad (14)$$

Hence, the difference (ΔDIC) between the expected initial DIC at IN-stations, $DIC_{IN(exp)}$, and that actually measured, $DIC_{IN(obs)}$, once corrected for air–sea gas exchange of CO_2 , results in the average rate of net biological uptake over the time period since eddy formation.

This approach was also applied to N+N, TOC and DON data to derive NCP. The equations are as follows:

$$\begin{aligned}
 NCP_{N+N} = & ((N + N)_{IN(exp)} - (N + N)_{IN(obs)}) \\
 & * \frac{H}{T} * (C/N)_{OM}
 \end{aligned} \quad (15)$$

$$\begin{aligned}
 NCP_{TOC} = & (TOC_{IN(obs)} - TOC_{IN(exp)}) \\
 & * \frac{H}{T} + F_{Export}
 \end{aligned} \quad (16)$$

$$\begin{aligned}
 NCP_{DON} = & ((DON)_{IN(obs)} - (DON)_{IN(exp)}) \\
 & * \frac{H}{T} * (C/N)_{DOM}
 \end{aligned} \quad (17)$$

where all the subscripts above have the same meaning as those in Eq. (14). For the N+N model, there is no air–sea exchange and nitrogen is converted to carbon assuming a C/N Redfield ratio of 6.6 (Redfield, 1958). For TOC, we must add an additional term, the POC export flux (F_{Export}) at the base of the defined water column (Williams, 1993). This flux was estimated for the eddy core using the average of the sediment trap and ^{234}Th -derived fluxes by Benitez-Nelson et al. (2007). For DON, N is converted into C assuming a much higher C/N ratio of 13.6 in dissolved organic matter (Benner et al., 1992). Please note that NCP from the DON mass balance does not include particle export at the bottom of the euphotic zone.

One caveat that we have yet to consider in the NCP determination based on DIC mass balance is possible carbonate removal due to biogenic calcium carbonate formation ($CaCO_3$ precipitation). There was no evidence of any significant growth of these types of organisms within Cyclone *Opal* (Brown et al., 2008; Landry et al., 2008; Rii et al., 2008). This was further supported by calculating a budget for dissolved calcium (data not shown) that indicated little to no difference between observed and expected calcium concentrations, $\sim 0.02 \text{ mmol kg}^{-1}$, well within the measurement error, and only minor changes in TALK between surface water and depth (Fig. 2F). We should also note that we did not include data from station IN1, as cast 49 at station IN1 was determined to be outside of the eddy core using ADCP data (Section 2.1).

5. Model results and discussion

5.1. NCP at OUT-stations

The average NCP and other net flux terms at three OUT-stations were estimated from the mass balances of DIC, N+N, TOC, and DON by using the mixed-layer model described in Section 4.1. Assuming negligible entrainment and horizontal advection and steady state (i.e. negligible time rate of change), mixed-layer NCP estimates from these mass balances are 5.63 ± 1.88 , 0.84 ± 0.16 , 1.89 ± 0.51 , and $0.78 \pm 0.35 \text{ mmol C m}^{-2} \text{ d}^{-1}$, respectively (Table 4). Significant uncertainties may be introduced to the individual flux

terms due to our model assumptions. For example, horizontal advection was ignored. In order to assess the magnitude of the horizontal advection term, we use DIC data collected during E-Flux II, across a southeast to northwest transect that included a region close in proximity to the OUT-stations (roughly the same location for E-Flux II and III). This transect showed a northwestward $nDIC$ gradient of $0.01 \pm 0.02 \text{ mmol C m}^{-3} \text{ km}^{-1}$. Assuming a net horizontal velocity of $\sim 2 \text{ cm s}^{-1}$ (Quay and Stutsman, 2003) results in a horizontal flux term of $1.64 \pm 3.30 \text{ mmol C m}^{-2} \text{ d}^{-1}$, which is about 30% of our initial estimate of NCP (Table 4). No similar measurements were conducted for TOC and DON. We should mention that for N+N, since it is always depleted in the mixed layer, likely has limited concentration gradients and thus significant horizontal advection is not expected.

The temporal stability of the biogeochemical properties in the absence of an eddy (OUT-stations) can be assessed by comparing the average DIC, salinity, N+N, TOC, and DON between E-Flux II and III cruises (Table 3). Since no mesoscale eddies were observed during E-Flux II (Dickey et al., 2008), all station data from this cruise, including stations collected in the eddy generation region, were compared to the data at E-Flux III OUT-stations. Overall, there are a ≤ 0.03 increase in salinity and $\leq 5 \text{ } \mu\text{mol kg}^{-1}$ increase in DIC in the mixed layer between E-Flux II and III. This increase is within the uncertainties of our measurement (Table 3). Furthermore, average $nDIC$ values over the upper 0–75 m (well within the mixed layer) during E-Flux II and E-Flux III are also the same within error (1959.0 ± 5.8 and $1962.4 \pm 4.5 \text{ } \mu\text{mol kg}^{-1}$, respectively). These results suggest that surface waters without the influence of eddies in the lee of Hawaiian Islands are quite stable within the winter season, which further justified our choice of E-Flux III OUT-stations as truly representative of the background, non-eddy impacted biogeochemistry of Hawaiian lee waters during E-Flux III. In order to assess the temporal impact on NCP budgets, we used an elapse time between the two cruises as ~ 2 months, and applied a small NCP correction factor (see Table 4).

After the adjustments of spatial and temporal change, NCP from the mass balance of DIC decreases from 5.63 ± 1.88 to $4.49 \pm 8.39 \text{ mmol C m}^{-2} \text{ d}^{-1}$. TOC-derived NCP, however, increases from 2.44 ± 1.00 to $3.37 \pm 1.11 \text{ mmol C m}^{-2} \text{ d}^{-1}$. Combined, the revised TOC and DIC estimates and the initial NCP estimates derived from N+N and DON, resulted in an average NCP of $2.37 \pm 4.24 \text{ mmol C m}^{-2} \text{ d}^{-1}$ at OUT-stations. In comparison, NCP at Station ALOHA, approximately 300 km north of our study area, ranges from 4.1 ± 0.8 to $7.4 \pm 4.7 \text{ mmol C m}^{-2} \text{ d}^{-1}$ over the mixed layer or euphotic zone (as summarized by Keeling et al. (2004)). Please note that NCP within the mixed layer is roughly 80% of NCP over the entire euphotic zone at Station ALOHA (Keeling et al., 2004). Our lower results appear reasonable given that the NCP estimates here are during the winter season (Quay and Stutsman, 2003; Keeling et al., 2004).

We did not conduct similar estimates for N+N and DON because mixed-layer N+N was depleted in both cruises and DON data were more complicated due to changes in composition, for example, preferential loss of specific nitrogen compounds during organic matter degradation (Benner et al., 1992). In addition, the results for N+N and DON must be converted to C by using C/N ratios (6.6 for N+N and 13.6 for DON), amplifying the errors significantly.

5.2. NCP at IN-stations

5.2.1. NCP calculations and the associated errors

To estimate NCP at IN-stations, we first applied the two end-member mixing model (described in Section 4.2) to calculate the

Table 4

OUT-stations ($n = 3$) NCP and other net carbon flux terms in the mixed layer (95 ± 7 m) from the budgets of DIC, N+N, TOC, and DON by using the mixed-layer model during E-Flux III

Term	Flux ($\text{mmol C m}^{-2} \text{d}^{-1}$)			
	DIC	N+N	TOC	DON
Air–sea CO_2 exchange ^a	2.90 ± 1.84	NA	NA	NA
Horizontal advection ^b	$0 (1.64 \pm 3.30)$	0	0	0
Vertical diffusion	2.73 ± 0.34	0.84 ± 0.16	0.64 ± 0.07	0.78 ± 0.35
POC export ^c	NA	NA	1.25 ± 0.51	NA
Time rate of change ^d	$0 (2.78 \pm 7.48)$	0	$0 (1.44 \pm 0.98)$	0
NCP	$5.63 \pm 1.88 (4.49 \pm 8.39)$	0.84 ± 0.16	$1.89 \pm 0.51 (3.33 \pm 1.11)$	0.78 ± 0.35

^a Only for the mixed layer DIC budget. This flux is from Chen et al. (2007).

^b Estimate only available for DIC budget.

^c Only for the mixed layer TOC budget. POC flux is from Benitez-Nelson et al. (2007).

^d The values in the brackets are estimated by using the difference of $n\text{DIC}$ between E-Flux II and II.

Table 5

Average observed and expected initial concentrations as well as the fraction of subtropical salinity maximum water (f_{deep}) over three depth horizons (0–50, 0–75, and 0–110 m) from two end-member mixing model at IN-stations and OUT-stations during E-Flux III

Stations	f_{deep} (%)	$\text{DIC}_{\text{IN(obs)}} (\mu\text{M})$	$\text{DIC}_{\text{IN(exp)}} (\mu\text{M})$	$\text{N+N}_{\text{IN(obs)}} (\mu\text{M})$	$\text{N+N}_{\text{IN(exp)}} (\mu\text{M})$	$\text{TOC}_{\text{IN(obs)}} (\mu\text{M})$	$\text{TOC}_{\text{IN(exp)}} (\mu\text{M})$	$\text{DON}_{\text{IN(obs)}} (\mu\text{M})$	$\text{DON}_{\text{IN(exp)}} (\mu\text{M})$
$\text{IN}_{\text{avg}} (0-50 \text{ m})$	67.6 ± 3.9	2031.6 ± 3.2	2046.9 ± 4.1	0.17 ± 0.12	1.14 ± 0.30	70.7 ± 2.3	63.1 ± 3.3	4.43 ± 0.40	3.88 ± 0.86
$\text{OUT}_{\text{avg}} (0-50 \text{ m})$	–	2002.9 ± 3.3	–	0.28 ± 0.08	–	73.2 ± 0.4	–	4.11 ± 0.05	–
$\text{IN}_{\text{avg}} (0-75 \text{ m})$	77.0 ± 5.7	2041.0 ± 3.1	2053.3 ± 5.3	0.31 ± 0.14	1.26 ± 0.37	68.9 ± 2.5	61.6 ± 4.0	4.34 ± 0.38	3.85 ± 0.84
$\text{OUT}_{\text{avg}} (0-75 \text{ m})$	–	2003.8 ± 4.6	–	0.25 ± 0.07	–	72.8 ± 0.3	–	4.09 ± 0.11	–
$\text{IN}_{\text{avg}} (0-110 \text{ m})$	83.1 ± 3.8	2053.5 ± 2.6	2056.8 ± 4.1	0.83 ± 0.14	1.33 ± 0.45	66.0 ± 2	60.5 ± 3.6	4.16 ± 0.24	3.84 ± 0.53
$\text{OUT}_{\text{avg}} (0-110 \text{ m})$	–	2007.6 ± 3.5	–	0.22 ± 0.05	–	71.9 ± 0.3	–	4.16 ± 0.13	–
$\text{OUT}_{\text{deep}} (150 \text{ m})$	–	2068.0 ± 3.3	–	1.51 ± 0.26	–	58.7 ± 1	–	3.78 ± 0.56	–

expected initial concentrations of DIC, N+N, TOC, and DON over three different depth horizons (0–50 m (the average MLD), 0–75 m (surface to DCML), and 0–110 m (the average euphotic zone)). In the mixed layer, uniform concentrations enable a simple mass balance of inputs and outputs. For the other two depth horizons above (0–75 and 0–110 m), however, non-uniform hydrographic and biogeochemical distributions complicate the calculation as different processes may affect distributions depending on their position in the water column. Nonetheless, we argue that a one-box, two end-member mixing model is still valid for determining the average and total NCP over a given depth horizon as long as the mixing components of a specific biogeochemical quantity are constrained using a salt budget. While this is likely true for the mixed layer and the 0–75 m depth horizon given the physics of Cyclone *Opal* (e.g., Nencioli et al., 2008), the 0–110 m depth integration at IN-stations should be viewed with caution as it includes the depth to which subtropical salinity maximum water extends (Nencioli et al., 2008).

Observed average concentrations at IN-stations, OUT-stations, and in the deep subtropical salinity maximum water are given in Table 5. These data, as well as the salinity data in Table 2, are used to calculate the expected IN-station initial concentrations and the fraction of the subtropical salinity maximum water within the desired depth horizons. Results are also presented in Table 5.

Using the two end-member mixing model described in Section 4.2, we determined average NCPs with uncertainty over three depth horizons. Specifics of the calculation of $\text{DIC}_{\text{IN(exp)}}$ in the mixed layer are given below as an example. According to Eq. (10), we first must determine the DIC concentration and salinity in the deep salinity maximum water, i.e. DIC_d and S_d , which are $2068.0 \pm 3.3 \mu\text{M}$ (converted from $\mu\text{mol kg}^{-1}$) and 35.122 ± 0.009 , respectively (Tables 2 and 5). DIC_{OUT} and S_{OUT} are $2002.9 \pm 3.3 \mu\text{M}$ and 34.882 ± 0.030 , respectively, while S_{IN} is 35.044 ± 0.013 . Thus,

f -value and $\text{DIC}_{\text{IN(exp)}}$ are calculated to be 68% and $2046.9 \pm 4.1 \mu\text{M}$, respectively (Table 5).

The error (1 SD uncertainty) of $\text{DIC}_{\text{IN(exp)}}$ depends on the errors in all the terms in Eq. (10). Sensitivity analyses suggest that changes of 1 SD uncertainty in the individual terms in Eq. (10) resulted in a $\text{DIC}_{\text{IN(exp)}}$ range of 1.1–3.5 μM . If the individual error terms are independent, an accumulated error of $\pm 5.2 \mu\text{M}$ is estimated. This results in an average difference between $\text{DIC}_{\text{IN(exp)}}$ and $\text{DIC}_{\text{IN(obs)}}$ (ΔDIC) of $15.3 \pm 5.2 \mu\text{M}$. Thus, although the error is large, the ΔDIC is still significant. Using this calculated change in DIC and the error in $F_{\text{air-sea}}$ in Eq. (14), we determined a NCP_{DIC} of $24.3 \pm 9.5 \text{ mmol C m}^{-2} \text{d}^{-1}$ for the mixed layer (Table 6A). We should mention that the NCP estimates here do not include the errors in terms of H and T in Eq. (14). The same strategy was used to determine differences between other observed and expected values (ΔDIC , $\Delta(\text{N+N})$, ΔTOC , and ΔDON over different depth horizons) and NCP from Eqs. (14) to (17) (Fig. 6 and Table 6).

Overall, the average differences between observed and expected values of the various biogeochemical constituents (ΔDIC , $\Delta(\text{N+N})$, ΔTOC , and ΔDON) decreased with increasing integration depths from 0–50 to 0–110 m, especially from 0–75 to 0–110 m. This trend suggests that the depletion of DIC and N+N and the accumulation of TOC and DON occurred mostly in the upper euphotic zone (above the DCML). Among these four biogeochemical parameters, the ΔDON has the greatest uncertainties over all the depth horizons. A major reason is that the decrease in DON with depth is relatively small and varies widely (Fig. 3F and Table 3). For the other three parameters, the differences between observed and expected values within the 0–50 and 0–75 m depth horizons are much larger than the calculated uncertainties. Over the 0–110 m depth horizon, however, smaller differences between observed and expected values resulted in significant relative errors (Fig. 6). Thus, the relative errors on the NCP calculation also increase with increasing depth integration (Table 6A–C). Please

Table 6
The average as well as individual IN-station NCP estimates over three depth horizons ((A): 0–50 m; (B): 0–75 m; and (C): 0–110 m) from two end-member mixing model and mass balances of DIC, N+N, TOC, and DON during E-Flux III

Stations	NCP _{DIC} (mmol C m ⁻² d ⁻¹)	NCP _{N+N} (mmol C m ⁻² d ⁻¹)	NCP _{TOC} (mmol C m ⁻² d ⁻¹)	NCP _{DON} (mmol C m ⁻² d ⁻¹)
(A) 0–50 m				
IN0	35.6 ± 19.6	10.4 ± 7.5	–	–
IN1	7.7 ± 12.2	–	–	–
IN2	30.5 ± 10.3	10.8 ± 7.6	19.6 ± 10.2	23.9 ± 11.5
IN3	27.4 ± 9.8	9.8 ± 7.4	12.3 ± 9	5.0 ± 10.4
IN4	27.2 ± 8.4	9.8 ± 7.4	11.4 ± 8.8	8.1 ± 10.6
IN5	44.2 ± 37.2	9.4 ± 7.4	10.9 ± 8.7	8.0 ± 10.6
IN6	18.3 ± 6.9	7.0 ± 6.9	11.1 ± 8.8	5.4 ± 10.4
IN7	–	8.8 ± 7.3	10.1 ± 8.6	11.9 ± 10.9
IN _{avg}	24.3 ± 9.5	9.1 ± 7.2	12.6 ± 9	10.7 ± 10.8
(B) 0–75 m				
IN0	36.3 ± 19.8	15.6 ± 8.4	–	–
IN1	3.9 ± 11.6	–	–	–
IN2	42.1 ± 14.4	15.1 ± 8.3	28.4 ± 11.7	33.3 ± 11.8
IN3	34.7 ± 11.8	12.6 ± 7.9	15.9 ± 9.6	5.8 ± 10.4
IN4	31.3 ± 11.2	15.7 ± 8.4	15.6 ± 9.5	15.3 ± 11.1
IN5	58.1 ± 17.8	14.2 ± 8.2	14.2 ± 9.3	9.7 ± 10.7
IN6	22.0 ± 10.3	11.1 ± 7.6	15.4 ± 9.5	6.9 ± 10.5
IN7	–	15.6 ± 8.9	15.4 ± 9.5	12.8 ± 10.9
IN _{avg}	28.6 ± 13.3	13.4 ± 7.9	17.6 ± 9.9	14.4 ± 11
(C) 0–110 m				
IN0	1.8 ± 11.2	11.5 ± 7.7	–	–
IN1	–14.7	–	–	–
IN2	26.4 ± 15.3	12.4 ± 7.8	31.1 ± 12.1	32.4 ± 11.8
IN3	24.4 ± 15	9.8 ± 7.4	15.8 ± 9.6	6.6 ± 10.5
IN4	19.4 ± 14.1	8.3 ± 7.2	13.3 ± 9.1	12.6 ± 10.9
IN5	58.8 ± 20.7	10.5 ± 7.5	15.1 ± 9.4	9.7 ± 10.7
IN6	7.3 ± 10.7	12.3 ± 7.8	19.5 ± 10.2	10.7 ± 10.8
IN7	–	14.4 ± 8.2	18.1 ± 10	12.0 ± 10.9
IN _{avg}	12.8 ± 13.1	10.5 ± 7.4	19.0 ± 10.1	14.1 ± 11

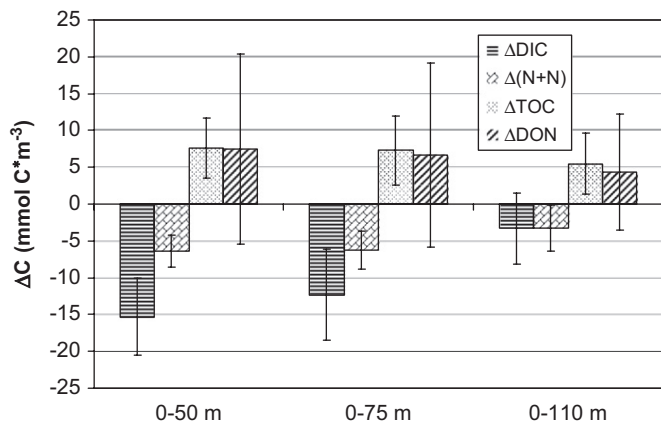


Fig. 6. Difference between average observed and expected concentrations of four biogeochemical parameters (Δ DIC, Δ (N+N), Δ TOC, and Δ DON) at IN-stations over three depth horizons (0–50, 0–75, and 0–110 m) from two end-member mixing model during E-Flux III. Please note that the unit of Δ (N+N) and Δ DON were converted to carbon by using different C/N ratios (6.6 and 13.6 for particulate organic carbon and dissolved organic carbon, respectively).

note that there is no substantial decrease in NCP estimates when integrated to deeper depths (0–110 m) as smaller values of Δ DIC, Δ (N+N), Δ TOC, and Δ DON are multiplied by a larger depth interval to obtain depth-integrated NCP.

NCP at individual IN-stations also was determined over the three depth horizons (0–50, 0–75, and 0–110) in order to assess the temporal variability and stability of estimates (Table 6A–C). Results suggest that NCP calculated by using N+N and TOC is substantially less variable than that by using DIC. This likely reflects the fact that the difference between observed and

expected DIC values is small relative to their background concentrations and associated uncertainties, especially with the increase of depth horizon. For example, Δ DIC over the 0–110 m depth horizon is $3.3 \pm 4.9 \mu\text{M}$. It is therefore difficult to distinguish the biological change in the DIC signal above the large background of DIC (Table 5). This problem is further confounded by the small salinity difference between surface and deep waters (Table 2). For example, sensitivity analyses suggest that a change of 0.01 in IN-station salinity (S_{IN}) or a $4 \mu\text{M}$ change in IN-station DIC ($\text{DIC}_{\text{IN}(\text{obs})}$) over the upper 0–110 m results in a significant difference in the estimated NCP of $\sim 100\%$. In contrast, the same change in S_{IN} only causes $\sim 20\text{--}30\%$ change in estimated NCP from N+N and TOC. Nevertheless, the in depth error analysis provided above, as well as the consistency in results using the various biogeochemical parameters, suggests that the NCP determined at the IN-stations reflects the general trend of enhanced NCP in the center of Cyclone *Opal*, especially within the mixed layer (0–50 m) and DCML (0–75 m) (Tables 6A–C).

We should mention that evaporation and precipitation were not explicitly included in the above calculations. Assuming a typical net evaporation rate of 435 mm yr^{-1} between 20°N and 30°N in the ocean (Peixoto and Oort, 1992) and an average mixed-layer depth of 50 m at IN-stations, the net influence of evaporation would result in an increase of 0.025 in salinity over the upper 50 m over a 1-month period. This is comparable to the observed increase in salinity between E-Flux II and E-Flux III OUT stations (Table 3). Applying this salinity adjustment to the IN and OUT stations in Eq. (7), the f -value would be reduced by 9% to 0.60. When this is applied to Eq. (10), however, DIC_{OUT} should equally be reduced to a lower pre-evaporation value. The resulting $\text{DIC}_{\text{IN}(\text{exp})}$ would be $4.7 \mu\text{M}$ lower. However, for an appropriate comparison with the $\text{DIC}_{\text{IN}(\text{obs})}$, this initial $\text{DIC}_{\text{IN}(\text{exp})}$ should also be subjected to evaporative concentration. Thus the final $\text{DIC}_{\text{IN}(\text{exp})}$ is

only 3.2 μM lower than the earlier calculation, which is significant, implying a 20% overestimation of our DIC-based NCP, but is still within the overall uncertainty due to other terms estimated earlier ($\pm 5.2 \mu\text{M}$). The above exercise is equivalent to the use of E-Flux II as the initial surface water end-member that has lower salinity and DIC values.

5.2.2. Vertical distribution of NCP

In the center of Cyclone *Opal*, higher carbon export is expected due to enhanced NCP and a shift in community structure from small pico-phytoplankton to large diatoms (Rii et al., 2008). The average NCPs (averaged from the mass balances of DIC, N+N, TOC, and DON) over the three depth horizons are 14.2 ± 9.2 (0–50 m), 18.5 ± 10.7 (0–75 m) and $14.1 \pm 10.6 \text{ mmol C m}^{-2} \text{ d}^{-1}$ (0–110 m), respectively (Table 6). These values are significantly higher than the average NCP at OUT-stations in the mixed layer ($\sim 0\text{--}95 \text{ m}$), $2.37 \pm 4.24 \text{ mmol C m}^{-2} \text{ d}^{-1}$. However, less than 15% of the average NCP in the euphotic zone was exported as POC below 150 m ($1.8 \pm 0.9 \text{ mmol C m}^{-2} \text{ d}^{-1}$, Benitez-Nelson et al. (2007)). The rest of the organic carbon production must either accumulate in the upper water column (0–110 m) as DOC or exported laterally. Contemporaneous measurements of suspended particulate C and particulate N indicate that TOC is mainly comprised of DOC (Landry et al., 2008; Mahaffey et al., 2008). Using the two end-member salt budget approach (Section 4.2), average observed TOC ($66.0 \pm 2.0 \mu\text{M}$) is $5.5 \mu\text{M}$ higher than the expected initial value ($60.5 \pm 3.6 \mu\text{M}$) over the upper 110 m (Table 5). Such a difference is equivalent, within error, to our average NCP estimates, suggesting that enhanced NCP was indeed stored in the upper water column as DOC.

To better understand the NCP throughout the water column, we plotted NCP over several different depth intervals (Fig. 7). Note that the NCP within the 50–75 m depth interval is actually the difference between the NCP over 0–75 m and that over 0–50 m. The same strategy is used to obtain NCP over the 75–110-m interval. Most of the NCP took place within the mixed layer (over 0–50 m depth horizon, Fig. 7). This is supported by the positive dissolved oxygen anomaly in the shallow euphotic zone of the eddy center (Nencioli et al., 2008). We should mention that no dissolved oxygen (DO) data from bottle samples were available for calibration. However, the intercomparison can still be done by using individual profiles (Nencioli et al., 2008).

In general, the upper two layers (0–50 and 50–75 m) maintained a positive NCP. The positive NCP within the mixed layer is consistent with modest increases in *Prochlorococcus* spp. and diatom abundance as well as the growth rates of *Prochlorococcus* spp. and other small phytoplankton, such as prymnesiophytes and pelagophytes (Landry et al., 2008; Rii et al., 2008). Positive NCP rates from 50 to 75 m is coincident with increased biomass and a shift in community structure from *Prochlorococcus* spp. to large ($> 20 \mu\text{m}$) diatoms (Landry et al., 2008). Above the DCML, in the upper 50–60 m, the diatom community was comprised of physiologically unhealthy diatoms with significantly depressed growth rates and proportionately greater grazing losses relative to the mixed layer and the DCML (Landry et al., 2008). Such an elevated biomass of diatoms between 50 m and the DCML confirms the intrusion of the deep nutrient-rich water and enhanced biological production after the initial isopycnal uplift of Cyclone *Opal*. It is further consistent with the positive NCP from 50 to 75 m, although there was no obvious growth rate enhancement due to Si limitation at the time of sample collection (Rii et al., 2008).

In contrast, the lower layer (75–110 m) had close to zero NCP. While diatom biomass and growth rates were still significant, large ($> 50 \mu\text{m}$) ciliates and dinoflagellates, the most likely protistan grazers of diatoms, were also ~ 3 times higher than ambient biomass levels (Brown et al., 2008). These consumers capture and process their food as individual prey items and produce individual empty frustules as a by-product of grazing (Jacobson and Anderson, 1996; Jeong et al., 2004; Landry et al., 2008). As such, they tend to produce smaller suspended particles and dissolved organic matter rather than large organically dense fecal pellets. These are consistent with the higher rates of remineralization implied below the DCML using $^{234}\text{Th}/^{238}\text{U}$ disequilibria and low rates of particle export (Maiti et al., 2008; Rii et al., 2008). Nonetheless, NCP may still be underestimated within 75–110 m. As mentioned in Section 4.2, there is solid body rotation down to $\sim 70 \text{ m}$ at the eddy center, essentially isolating this water mass from the surrounding waters. Below 70 m, mixing along isopycnal surfaces may have occurred, allowing the horizontal intrusion of deep nutrient-rich water at the eddy center. Thus the age of water mass within the lower layer (75–110 m) may have been much younger than the assumed

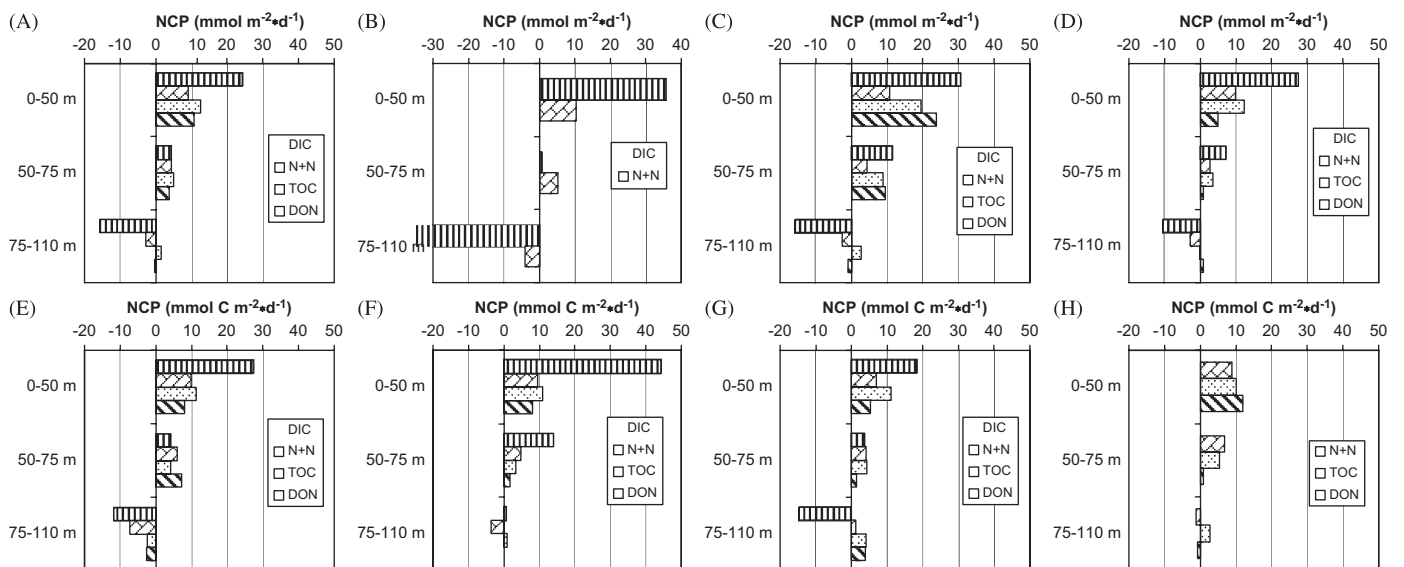


Fig. 7. Net community production (NCP) based on DIC, N+N, TOC, and DON mass balance by using salt budget approach at three different depth intervals: 0–50, 50–75, and 75–110 m, respectively: (A) average NCP estimate at IN-stations; and (B–H) NCP estimates at individual IN-stations.

elapse time, which is ~ 35 days (Dickey et al., 2008; Nencioli et al., 2008).

NCP from TOC mass balance is likely a conservative estimate (Eq. (16); Tables 6A–C and Fig. 7) in that we applied the carbon export flux at 150 m to shallower depth intervals (0–50, 0–75, and 0–110 m). However, we would expect higher carbon export fluxes at shallower depths since carbon export fluxes generally decrease with depth as well (Cochran et al., 1993; Amiel et al., 2002). Please note that NCP estimated from TOC mass balance in the lower layers (75–110 m) shows small positive values at IN-stations (IN2: Fig. 7C, IN5: Fig. 7F, IN6: Fig. 7G, IN7: Fig. 7H, and the average NCP in Fig. 7A).

6. Conclusions and significance

This study examined how a wind-driven cyclonic eddy, Cyclone *Opal*, influenced NCP. NCP estimates from mass balances of salt, DIC, N+N, TOC, and DON consistently suggest that on average, there was substantially enhanced NCP in the center of the eddy relative to that in the surrounding waters. In the average mixed layer (0–50 m) of the eddy center, NCP was $14.2 \pm 9.2 \text{ mmol C m}^{-2} \text{ d}^{-1}$; within the DCML (~ 0 –75 m), NCP was $18.5 \pm 10.7 \text{ mmol C m}^{-2} \text{ d}^{-1}$; and for the euphotic zone, NCP was $14.1 \pm 10.6 \text{ mmol C m}^{-2} \text{ d}^{-1}$. In contrast, NCP for the mixed layer was $2.37 \pm 4.24 \text{ mmol C m}^{-2} \text{ d}^{-1}$ outside the eddy. Enhanced NCP in the center of Cyclone *Opal* is consistent with earlier studies that NP depends on mixing and vertical advection processes (Eppley and Peterson, 1979; Mourino and McGillicuddy, 2006). Our models may involve significant uncertainties due to the lack of knowledge of initial conditions and future efforts should strive to incorporate additional biogeochemical constraints wherever possible. For example, NCP using a DIC budget would have been better estimated with the additional $\delta^{13}\text{C}$ -DIC estimates. In addition, efforts should be made to include all of the mass balance terms with better error control, even if less significant (see values in the brackets, Table 4).

Subtropical gyres show seasonal metabolic variation in the upper water column (Williams et al., 2004; Juranek and Quay, 2005). In situ NCP on four cruises to the Hawaii Ocean Time series (HOT) Station ALOHA during 2002–2003 was estimated to $\sim 10 \text{ mmol C m}^{-2} \text{ d}^{-1}$ in the summer (Juranek and Quay, 2005). However, a neutral or net heterotrophic state was indicated by the winter data. Quay and Stutsman (2003) also determined much higher NCP at Station ALOHA during the summer, which is $7.2 \pm 2.9 \text{ mmol C m}^{-2} \text{ d}^{-1}$. Such net autotrophy in summer and net heterotrophy in winter was also suggested during a series of HOT cruises between May 2001 and May 2002 (Williams et al., 2004). Our NCP estimates in the center of the eddy are higher than the above NCP results in the subtropical Pacific Ocean in summer. Considering that our March cruise occurred during the winter, this comparison also indirectly supports the view that NCP is substantially enhanced due to mesoscale eddies, although mechanisms of NCP enhancement may differ from those at Station ALOHA over the summer. Such an enhanced NCP is also consistent with studies that mesoscale eddy-driven events are likely major mechanisms for supplying new nutrient to the upper ocean and hence, increased PP (McGillicuddy and Robinson, 1997; McGillicuddy et al., 1998).

Our results suggest that the euphotic zone can be further divided into two layers: an upper layer (0–75 m) that is characterized with positive NCP and a lower layer (75–110 m) with NCP rates not significantly different from zero. Inside Cyclone *Opal*, enhanced NCP and shifting community structure (from pico-phytoplankton to diatoms) suggested that a higher carbon export would be observed. Surprisingly, most of the

enhanced NCP was stored in the surface water as DOC rather than exported as POC to the deep ocean. This suggests that eddies are not necessarily more efficient in exporting particulate organic matter to deep waters.

Acknowledgements

We thank all E-Flux collaborators, especially T. Dickey, W. Black, F. Nencioli, K. Maiti, P. McAndrew, J. Becker, T. Bibby, and Michael Landry's group for their help to access the shipboard data and sampling collection, and G. Han for her laboratory support for DIC analysis. We thank the crew of the *Wecoma* for logistical support, and D. McGillicuddy and three anonymous reviewers for their comments and editorial helps that greatly improved this manuscript. This work was supported by an NSF Grant (OCE-0241645) to C.R. Benitez-Nelson and an NSF Grant (OCE-0425153) to W.-J. Cai.

References

- Allen, C.B., Kanda, J., Laws, E.A., 1996. New production and photosynthetic rates within and outside a cyclonic mesoscale eddy in the North Pacific subtropical gyre. *Deep-Sea Research Part I—Oceanographic Research Papers* 43, 917–936.
- Amiel, D., Cochran, J.K., Hirschberg, D.J., 2002. $\text{X}^{234}\text{Th}/^{238}\text{U}$ disequilibrium as an indicator of the seasonal export flux of particulate organic carbon in the North Water (The International North Water Polynya Study). *Deep-Sea Research Part II—Topical Studies in Oceanography* 49 (22–23), 5191–5209.
- Anderson, R.A., Bidigare, R.R., Keller, M.D., Latasa, M., 1996. A comparison of HPLC pigment signatures and electron microscopic observations for oligotrophic waters of the North Atlantic and Pacific Oceans. *Deep-Sea Research Part II—Topical Studies in Oceanography* 43, 517–537.
- Benitez-Nelson, C.R., Bidigare, R.R., Dickey, T., Landry, M.R., Leonard, C.L., Brown, S.L., Nencioli, F., Rii, Y.M., Maiti, K., Becker, J.W., Bibby, T.S., Black, W., Cai, W.-J., Carlson, C., Chen, F., Kuwahara, V.S., Mahaffey, C., McAndrew, P.M., Quay, P.D., Rappe, M., Selph, K.E., Simmons, M.P., Yang, E.J., 2007. Mesoscale eddies drive increased silica export in the subtropical Pacific Ocean. *Science* 316, 1017–1021.
- Benner, R., Pakilski, J.D., McCarthy, M., Hedges, J.I., Hatcher, P.G., 1992. Bulk chemical characteristics of dissolved organic matter in the ocean. *Science*, 1561–1564.
- Bidigare, R.R., Benitez-Nelson, C., Leonard, C.L., Quay, P.D., Parsons, M.L., Foley, D.G., Seki, M.P., 2003. Influence of a cyclonic eddy on microheterotroph biomass and carbon export in the lee of Hawaii. *Geophysical Research Letters* 30 (6), 1318.
- Broenkow, W.W., 1965. The distribution of nutrients in the Costa Rica Dome in the eastern tropical Pacific Ocean. *Limnology and Oceanography* 10, 40–52.
- Brown, S.L., Yang, E.J., Landry, M.R., Selph, K., 2008. Diatoms in the dissert. *Deep-Sea Research Part II*, this issue.
- Cai, W.-J., Wang, Y., 1998. The chemistry, fluxes and sources of carbon dioxide in the estuarine waters of the Satilla and Altamaha Rivers, Georgia. *Limnology and Oceanography* 43, 657–668.
- Capone, D.G., Zehr, J.P., Paerl, H.W., Bergman, B., Carpenter, E.J., 1997. *Trichodesmium*, a globally significant marine cyanobacterium. *Science* 276 (5316), 1221–1229.
- Carlson, C.A., Giovannoni, S.J., Hansell, D.A., Goldberg, S.J., Parsons, R., Vergin, K., 2004. Interactions between DOC, microbial processes, and community structure in the mesopelagic zone of the northwestern Sargasso Sea. *Limnology and Oceanography* 49, 1073–1083.
- Chavanne, C., Flament, P., Lumpkin, R., Dousset, B., Bentamy, A., 2002. Scatterometer observations of wind variations by oceanic islands: implications for wind driven ocean circulation. *Canadian Journal of Remote Sensing* 28 (3), 466–474.
- Chen, F., Cai, W.-J., Benitez-Nelson, C., Wang, Y., 2007. Sea surface pCO_2 -SST relationships across a cold-core cyclonic eddy: implications for understanding regional variability and air-sea gas exchange. *Geophysical Research Letters* 34 (L10603).
- Chierici, M., Miller, L.A., Whitney, F.A., Johnson, K.W., Wong, C.S., 2005. Biogeochemical evolution of the carbon dioxide system in the waters of long-lived mesoscale eddies in the Northeast Pacific Ocean. *Deep-Sea Research Part II—Topical Studies in Oceanography* 52 (7–8), 955–974.
- Cochran, J.K., Buesseler, K.O., Bacon, M.P., Livingston, H.D., 1993. Thorium isotopes as indicators of particle dynamics in the upper ocean: results from the JGOFS North Atlantic Bloom experiment. *Deep-Sea Research Part I—Oceanographic Research Papers* 40 (8), 1569–1595.
- Crawford, W.R., Whitney, F., 1999. Mesoscale eddies swirl with data in Gulf of Alaska Ocean. *EOS, Transactions, American Geophysical Union* 80, 365–370.
- Denman, K., Gargett, A., 1983. Time and space scales of vertical mixing and advection of phytoplankton in the upper ocean. *Limnology and Oceanography* 28 (5), 801–805.

- Dickey, T., Marra, J., Sigurdson, D.E., Weller, R.A., Kinkade, C.S., Zedler, S.E., Wiggert, J.D., Langdon, C., 1998. Seasonal variability of bio-optical and physical properties in the Arabian Sea: October 1994–October 1995. *Deep-Sea Research Part II—Topical Studies in Oceanography* 45, 2001–2025.
- Dickey, T., Nencioli, F., Kuwahara, V.S., Leonard, C.L., Black, W., Bidigare, R.R., Rii, Y.M., Zhang, Q., 2008. Physical and bio-optical observations of oceanic cyclones west of the Island of Hawaii. *Deep-Sea Research Part II*, this volume [doi:10.1016/j.dsr2.2008.01.006].
- Dickson, A.G., Millero, F., 1987. A comparison of the equilibrium constants for the dissolution of carbonic acid in seawater media. *Deep-Sea Research Part A—Oceanographic Research Papers* 34, 1733–1743.
- Dugdale, R.C., Goering, J.J., 1967. Uptake of new and regenerated forms of nitrogen in primary productivity. *Limnology and Oceanography* 12, 196–206.
- Eppley, R.W., Peterson, B.J., 1979. Particulate organic matter flux and planktonic new production in the deep ocean. *Nature* 282, 677–680.
- Falkowski, P.G., Ziemann, D., Kolber, Z., Bienfang, P.K., 1991. Role of eddy pumping in enhancing primary production in the ocean. *Nature* 352 (6330), 55–58.
- Fischer, A.S., Weller, R.A., Rudnick, D.L., Lee, C.C., Brink, K.H., Fox, C.A., Leben, R.R., 2002. Mesoscale eddies, coastal upwelling, and the upper-ocean heat budget in the Arabian Sea. *Deep-Sea Research Part II—Topical Studies in Oceanography* 49 (12), 2231–2264.
- Gordon, L.L., Jennings, J.C., Ross, A.A., Krest, J.M., 1994. A suggested protocol for continuous flow analysis of seawater nutrients (phosphate, nitrate, nitrite, and silicic acid) in the WOCE Hydrographic Program and Joint Global Ocean Fluxes Study. *WHP Office Report* 91-1.
- Gruber, N., Keeling, C.D., Stocker, T.F., 1998. Carbon-13 constraints on the seasonal inorganic carbon budget at the BATS site in the northwestern Sargasso Sea. *Deep-Sea Research Part I—Oceanographic Research Papers* 45 (4–5), 673–717.
- Haury, L.R., 1984. An offshore eddy in the California current system Part IV: plankton distributions. *Progress in Oceanography* 13, 95–111.
- Honjo, S., Dymond, J., Prell, W., Ittekkot, V., 1999. Monsoon-controlled export fluxes to the interior of the Arabian Sea. *Deep-Sea Research Part II—Topical Studies in Oceanography* 46 (8–9), 1859–1902.
- Jacobson, D.M., Anderson, D.M., 1996. Widespread phagocytosis of ciliates and other protists by marine mixotrophic and heterotrophic thecate dinoflagellates. *Journal of Phycology* 32 (2), 279–285.
- Jenkins, W.J., Goldman, J.C., 1985. Seasonal oxygen cycling and primary production in the Sargasso Sea. *Journal of Marine Research* 43 (2), 465–491.
- Jeong, H.J., Yoo, Y.D., Kim, S.T., Kang, N.S., 2004. Feeding by the heterotrophic dinoflagellate *Protoperidinium bipes* on the diatom *Skeletonema costatum*. *Aquatic Microbial Ecology* 36 (2), 171–179.
- Juraneck, L.W., Quay, P.D., 2005. In vitro and in situ gross primary and net community production in the North Pacific Subtropical Gyre using labeled and natural abundance isotopes of dissolved O₂. *Global Biogeochemical Cycles* 19 (GB3009).
- Keeling, C.D., Brix, H., Gruber, N., 2004. Seasonal and long-term dynamics of the upper ocean carbon cycle at Station ALOHA near Hawaii. *Global Biogeochemical Cycles* 18 (GB4006).
- Landry, M.R., Brown, S.L., Rii, Y.M., Selph, K.E., Bidigare, R.R., Yang, E.J., Simmons, M.P., 2008. Depth-stratified phytoplankton dynamics in Cyclone *Opal*, a subtropical mesoscale eddy. *Deep-Sea Research Part II*, this volume [doi:10.1016/j.dsr2.2008.02.001].
- Lee, K., 2001. Global net community production estimated from the annual cycle of surface water total dissolved inorganic carbon. *Limnology and Oceanography* 46 (6), 1287–1297.
- Letelier, R.M., Karl, D.M., Abbott, M.R., Flament, P., Freilich, M., Lukas, R., Strub, T., 2000. Role of later winter mesoscale events in the biogeochemical variability of the upper water column of the North Pacific Subtropical Gyre. *Journal of Geophysical Research—Oceans* 105 (C12), 28723–28740.
- Li, Y.-H., Karl, D.M., Winn, C.D., Mackenzie, F.T., Gans, K., 2000. Remineralization ratios in the subtropical North Pacific gyre. *Aquatic Geochemistry* 6, 65–86.
- Lumpkin, C.F., 1998. Eddies and currents of the Hawaiian Islands. Ph.D. Dissertation, University of Hawaii, 281pp.
- Mahaffey, C., Benitez-Nelson, C.R., Bidigare, R.R., Rii, Y.M., Karl, D.M., 2008. Nitrogen dynamics within a wind-driven eddy. *Deep-Sea Research Part II*, this volume [doi:10.1016/j.dsr2.2008.02.004].
- Maiti, K., Benitez-Nelson, C.R., Rii, Y.M., Bidigare, R.R., 2008. The influence of a mature cyclonic eddy on particle export in the lee of Hawaii. *Deep-Sea Research Part II*, this volume [doi:10.1016/j.dsr2.2008.02.008].
- McGillicuddy Jr., D.J., Robinson, A.R., 1997. Eddy-induced nutrient supply and new production in the Sargasso Sea. *Deep-Sea Research Part I—Oceanographic Research Papers* 44 (8), 1427–1450.
- McGillicuddy Jr., D.J., Robinson, A.R., Siegel, D.A., Jannasch, H.W., Johnson, R., Dickey, T.D., McNeil, J., Michaels, A.F., Knap, A.H., 1998. Influence of mesoscale eddies on new production in the Sargasso Sea. *Nature* 394 (6690), 263–266.
- McGillicuddy Jr., D.J., Anderson, D.J., Doney, S.C., Maltrud, M.E., 2003. Eddy-driven sources and sinks of nutrients in the upper ocean: results from a 0.1° resolution model of the North Atlantic. *Global Biogeochemical Cycles* 17 (2), 1035.
- McGillicuddy Jr., D.J., Anderson, L.A., Bates, N.R., Bibby, T., Buesseler, K.O., Carlson, C.A., Davis, C.S., Ewart, C., Falkowski, P.G., Goldthwait, S.A., Hansell, D.A., Jenkins, W.J., Johnson, R., Kosnyrev, V.K., Ledwell, J.R., Li, Q.P., Siegel, D.A., Steinberg, D.K., 2007. Eddy/wind interactions stimulate extraordinary mid-ocean plankton blooms. *Science* 316, 1021–1026.
- McNeil, J.D., Jannasch, H.W., Dickey, T., McGillicuddy, D., Brzezinski, M., Sakamoto, C.M., 1999. New chemical, bio-optical and physical observations of upper ocean response to the passage of a mesoscale eddy off Bermuda. *Journal of Geophysical Research—Oceans* 104 (C7), 15537–15548.
- Mehrbach, C., Cuberson, C.H., Hawley, J.E., Pytkowicz, R.M., 1973. Measurement of the apparent dissociation constants of carbonic acid in seawater at atmospheric pressure. *Limnology and Oceanography* 18, 897–907.
- Minas, H.J., Minas, M., Packard, T.T., 1986. Productivity in upwelling areas deduced from hydrographic and chemical fields. *Limnology and Oceanography* 31 (6), 1182–1206.
- Mourino, C.B., McGillicuddy Jr., D.J., 2006. Mesoscale variability in the metabolic balance of the Sargasso Sea. *Limnology and Oceanography* 51 (6), 2675–2689.
- Nencioli, F., Kuwahara, V.S., Dickey, T., Rii, Y.M., Bidigare, R.R., 2008. Physical dynamics and biological implications of a mesoscale eddy in the lee of Hawaii: Cyclone *Opal* observations during E-Flux III. *Deep-Sea Research Part II*, this volume [doi:10.1016/j.dsr2.2008.02.003].
- Officer, C.B., 1980. Box model revisited. In: Hamilton, P., Macdonald, K.B. (Eds.), *Estuarine and Wetland Processes*. Plenum Press, New York.
- Olaizola, M., Ziemann, D.A., Bienfang, P.K., Walsh, W.A., Conquest, L.D., 1993. Eddy-induced oscillations of the pycnocline affect the floristic composition and depth distribution of phytoplankton in the subtropical Pacific. *Marine Biology* 116, 533–542.
- Oschlies, A., 2002. Can eddies make ocean deserts bloom? *Global Biogeochemical Cycles* 16(4), 1106, doi:1110.1029/2001GB001830.
- Oschlies, A., Garçon, V., 1998. Eddy-induced enhancement of primary production in a model of the North Atlantic Ocean. *Nature* 394, 266–269.
- Patzert, W.C., 1969. Eddies in Hawaiian Islands. Report no. HIG-69-8, Hawaii Institute of Geophysics, University of Hawaii, Honolulu, HI.
- Peixoto, J.P., Oort, A.H., 1992. Observed mean state of the atmosphere. In: *Physics of Climate*. American Institute of Physics, New York, pp. 131–175.
- Platt, T., Harrison, W.G., Lewis, M.R., Li, W.K.W., Sathyendranath, S., Smith, R.E., Vezina, A.F., 1989. Biological production in the oceans: the case for a consensus. *Marine Ecology Progress Series* 52, 77–88.
- Quay, P., Stutsman, J., 2003. Surface layer carbon budget for the subtropical N. Pacific: $\delta^{13}\text{C}$ constraints at Station ALOHA. *Deep-Sea Research Part I—Oceanographic Research Papers* 50 (9), 1045–1061.
- Redfield, A.C., 1958. The biological control of chemical factors in the environment. *American Science* 46, 206–226.
- Rii, Y.M., Brown, S.L., Nencioli, F., Kuwahara, V.S., Dickey, T.D., Karl, D.M., Bidigare, R.R., 2008. The transient oasis: nutrient–phytoplankton dynamics and particle export in Hawaiian lee cyclones. *Deep-Sea Research Part II*, this volume [doi:10.1016/j.dsr2.2008.01.013].
- Sabine, C.L., Mackenzie, F.T., Winn, C., Karl, D.M., 1995. Geochemistry of carbon dioxide in seawater at the Hawaii Ocean time series station, ALOHA. *Global Biogeochemical Cycles* 9 (4), 637–651.
- Savidge, G., Williams, P.J.L.B., 2001. The PRIME 1996 cruise: an overview. *Deep-Sea Research II* 48, 687–704.
- Seki, M.P., Polovina, J.J., Brainard, R.E., Bidigare, R.R., Leonard, C.L., Foley, D.G., 2001. Biological enhancement at cyclonic eddies tracked with GOES thermal imagery in Hawaiian waters. *Geophysical Research Letters* 28 (8), 1583–1586.
- Shulenberger, E., Reid, J.L., 1981. The Pacific shallow oxygen maximum, deep chlorophyll maximum, and primary productivity, reconsidered. *Deep-Sea Research* 28, 901–920.
- Siegel, D.A., McGillicuddy Jr., D.J., Fields, E.A., 1999. Mesoscale eddies, satellite altimetry, and new production in the Sargasso Sea. *Journal of Geophysical Research—Oceans* 104 (C6), 13359–13379.
- Sweeney, E.N., McGillicuddy, J.D.J., Buesseler, K.O., 2003. Biogeochemical impacts due to mesoscale eddy activity in the Sargasso Sea as measured at the Bermuda Atlantic Time-series Study (BATS). *Deep-Sea Research Part II—Topical Studies in Oceanography* 50 (22–26), 3017–3039.
- Vaillancourt, R.D., Marra, J., Seki, M.P., Parsons, M.L., Bidigare, R.R., 2003. Impact of a cyclonic eddy on phytoplankton community structure and photosynthetic competency in the subtropical North Pacific Ocean. *Deep-Sea Research Part I—Oceanographic Research Papers* 50 (7), 829–847.
- Wang, Z.A., Cai, W.J., 2004. Carbon dioxide degassing and inorganic carbon export from a marsh-dominated estuary (the Duplin River): a marsh CO₂ pump. *Limnology and Oceanography* 49 (2), 341–354.
- Williams, P.J.L.B., 1993. On the definition of plankton production terms. *ICES Marine Science Symposium* 197, 9–19.
- Williams, R.G., Follows, M.J., 1998. Eddies make ocean deserts bloom. *Nature* 394, 228–229.
- Williams, P.J.L.B., Morris, P.J., Karl, D.M., 2004. Net community production and metabolic balance at the oligotrophic ocean site, Station ALOHA. *Deep-Sea Research Part I—Oceanographic Research Papers* 51, 1563–1578.
- Winn, C.D., Mackenzie, F.T., Carrillo, C.J., Sabine, C.L., Karl, D.M., 1994. Air–sea carbon dioxide exchange in the North Pacific Subtropical Gyre: implications for the global carbon budget. *Global Biogeochemical Cycles* 8 (2), 157–163.
- Wyrтки, K., Kilonsky, B., 1984. Mean water and current structure during the Hawaii–Tahiti shuttle experiment. *Journal of Physical Oceanography* 14, 242–254.